Technological University Dublin

ARROW@TU Dublin

2022-05-16

Contributions of Vibrational Spectroscopy to Virology: A Review

Iqra Chaudhary
Technological University Dublin

Naomi Jackson
Technological University Dublin

Denise Denning
Technological University Dublin

See next page for additional authors

Recommended Citation

Authors

Iqra Chaudhary, Naomi Jackson, Denise Denning, Luke O'Neill, and Hugh Byrne

Journal Pre-proof

Contributions of Vibrational Spectroscopy to Virology: A Review

Iqra Chaudhary, Naomi Jackson, Denise Denning, Luke O'Neill, Hugh J. Byrne

Please cite this article as: Iqra Chaudhary, Naomi Jackson, Denise Denning, Luke O'Neill and Hugh J. Byrne, Contributions of Vibrational Spectroscopy to Virology: A Review, *Clinical Spectroscopy,* (2022) doi:https://doi.org/10.1016/j.clispe.2022.100022

This is a PDF file of an article that has undergone enhancements after acceptance, such as the addition of a cover page and metadata, and formatting for readability, but it is not yet the definitive version of record. This version will undergo additional copyediting, typesetting and review before it is published in its final form, but we are providing this version to give early visibility of the article. Please note that, during the production process, errors may be discovered which could affect the content, and all legal disclaimers that apply to the journal pertain.

Contributions of Vibrational Spectroscopy to Virology: A Review

Iqra Chaudhary[1,2#], Naomi Jackson[1,2#], Denise Denning[1], Luke O'Neill[1], Hugh J. Byrne[1]*

FOCAS Research Institute, Technological University Dublin, City Campus, Camden Row, Dublin 8, Ireland

School of Physics and Clinical & Optometric Sciences, Technological University Dublin, City Campus, Grange Gorman, Dublin 7, Ireland

Joint first authors

* Corresponding author: Hugh.Byrne@TUDublin.ie

Abstract:

Vibrational spectroscopic techniques, both infrared absorption and Raman scattering, are high precision, label free analytical techniques which have found applications in fields as diverse as analytical chemistry, pharmacology, forensics and archeometrics and, in recent times, have attracted increasing attention for biomedical applications. As analytical techniques, they have been applied to the characterisation of viruses as early as the 1970s, and, in the context of the coronavirus disease 2019 (COVID-19) pandemic, have been explored in response to the World Health Organisation as novel methodologies to aid in the global efforts to implement and improve rapid screening of viral infection. This review considers the history of the application of vibrational spectroscopic techniques to the characterisation of the morphology and chemical compositions of viruses, their attachment to, uptake by and replication in cells, and their potential for the detection of viruses in population screening, and in infection response monitoring applications. Particular consideration is devoted to recent efforts in the detection of severe acute respiratory syndrome coronavirus 2, and monitoring COVID-19.

Keywords: Vibrational spectroscopy; infrared absorption spectroscopy; Raman spectroscopy; virus

1. Introduction:

Viruses have existed for billions of years, coexisting with humans in a battle of disease versus eradication, as was successfully achieved for smallpox. We, as humans, have lived alongside viruses and have attempted to combat some of the associated diseases by developing protection methods such as vaccines and antiviral therapeutics. However, viruses rapidly evolve, as evident by the new Severe Acute Respiratory Syndrome Coronavirus 2 (SARS-CoV-2) viral strain, which in 2020 effectively brought the world to a halt [1]. However, this was not the first time in human history the detrimental effects a virus can have on society was seen. The Spanish flu swept across the globe killing millions of people in the 1920s, and similarly the human immunodeficiency virus (HIV) pandemic has killed more than 35 million individuals to date [2].

In light of the recent pandemic, it is clear that there remain many knowledge gaps in our understanding of the mechanisms of viral infection, replication and host response, and shortcomings in methodologies available to analyse and characterise them. In February 2020, in response to the outbreak of the pandemic, the World Health Organisation (WHO), in collaboration with the Global Research Collaboration for Infectious Disease Preparedness and Response (GLOPID-R), organised a Global Forum on research and innovation for COVID19, and published a Global Research Roadmap to promote a co-ordinated approach to address the emerging global crisis [3]. The report recognises that there are major gaps in our understanding of many key aspects of the evolution, transmission, and effects of viruses, and in areas of diagnostics and therapeutics. It emphasises the importance of improved fundamental understanding of the processes associated with viral infection and advocates the development of new tools to monitor, for example, phenotypic change and potential adaptation,

not just in the context of the SARS-CoV-2 outbreak, but to support responses to other ongoing or future outbreaks across the world.

Vibrational Spectroscopic techniques, such as Raman and Infrared (IR) absorption, are powerful analytical tools and their potential role in medical diagnostics is being increasingly explored [4–6]. The spectrum obtained from these techniques comprises contributions from each molecular bond, and is a "signature" or "fingerprint" which is characteristic of a material, or changes associated with a physical or chemical process. In complex samples, notably biological cells or tissue, the spectroscopic signature incorporates characteristics of all constituent functional groups of lipids, carbohydrates, proteins, nucleic acids, and provides a high content, holistic representation of the biochemical status, which can be monitored as a function of time, to understand the kinetics of processes [7,8]. In cytology, vibrational spectroscopic microscopy has emerged as a label free alternative to conventional labelled techniques, which can provide molecularly specific signatures of biological processes and function [8]. Importantly, label free spectroscopic analysis can identify signatures of subcellular phenomena not evident in a labelled approach, which assumes *a priori* knowledge of specific molecular biomarkers. It can thus potentially guide the identification of new biomarkers of cellular events, or recognition of phenomena not visible using other, for example fluorescence based techniques [9]. These techniques have been extensively explored to differentiate between healthy and diseased samples for diagnostic applications [10–13], and recent studies using Raman and IR absorption spectroscopy have demonstrated great potential for their use with liquid biopsies samples [14–17].

As analytical and potential biomedical techniques, Raman and IR absorption spectroscopies have also been explored for the characterisation and detection of viruses, to monitor their cellular interactions and replication, and to diagnose and quantify viral infection. Based on a Web of Science literature search (November 2021) of abstracts containing the terms (Raman) OR (surface-enhanced Raman) OR (SERS) OR (Infrared) OR (FTIR) OR (MIR) OR (ATR)) AND (spectroscopy) AND (virus OR viral) NOT ("Near" OR NIR), this paper seeks to review the history and current state of the art of the application of Raman and (mid) IR spectroscopies in the field of analysis and characterisation of viruses, their cellular interactions, and human responses to infection. A brief introduction to the spectroscopic techniques considered in scope is first provided, after which the contributions of vibrational spectroscopy to characterisation of the structure and composition of viruses, their cellular interactions, and monitoring infection and physiological responses are reviewed. Against this backdrop, the recent efforts to aid in the global efforts to implement and improve rapid screening of viral infection to control the COVID-19 pandemic are discussed, and the future perspectives considered.

2. Vibrational Spectroscopy:

Vibrational spectroscopy measures transitions between the quantised vibrational states of molecules or solids, by absorption or scattering of incident radiation, and the spectrum of spectroscopic responses is characteristic of the material, of changes to it [18]. The transition energies are typically in the mid infrared (mid-IR) region of the spectrum (~400-4000 cm^{-1}), and thus are commonly directly measured by (Fourier Transform) IR absorption spectroscopy, or via their overtone/combination modes in the near-IR region. In the microscopic mode, the spatial resolution of the measurement is largely limited by the measurement wavelength (~2-20 μm), which can be optimised using well collimated sources, such as synchrotron or quantum cascade lasers (QCL), the enhanced brightness of which has also been exploited for the measurement of, for example, spectra of live cells in the highly absorbing aqueous *in vitro* cell culture media [19,20]. Emerging techniques have coupled scanning probe microscopy to detect IR induced photothermal and near field responses, and have opened up the potential to probe IR spectroscopic profiles with lateral resolution on a scale of tens of nanometers [21,22].

Raman spectroscopy, based on the inelastic scattering of light due to coupling with the vibrational modes of a material, is commonly performed at visible or near-IR wavelengths, and the lower intrinsic spatial resolution of ~0.5 μm, coupled with the fact that water is relatively weaker in Raman than in IR, means that confocal Raman microscopy lends itself more naturally to cellular and subcellular analysis [8], and has been employed, for example, to monitor the uptake, transport and cellular response to nanoparticles [23,24] and chemotherapeutic agents [25]. Combining the spatial resolution of atomic force microscopy with the chemical specificity of Raman spectroscopy, tip enhanced Raman spectroscopy (TERS) enables nanometer scale chemical imaging of surfaces [26]. Using plasmonically active TERS probes, the sensitivity is significantly enhanced by the surface enhanced Raman scattering (SERS) effect [27,28] through enhanced local fields in the vicinity of the metallic surface plasmon resonances. The enhancement is localised to within ~10 nm of the metal surface, and therefore is exhibited only by molecules in close proximity to it.

Not requiring spatial resolution, the applications of vibrational spectroscopy for quantitative analysis of metabolites in, and disease diagnostics based on biofluids [29–32], including blood [16,33], urine [34] and saliva [35–39], have become increasingly prevalent over the past decade. Attenuated total reflection FTIR (ATR-FTIR) in particular has emerged as a potentially viable option for clinical translation, as a rapid clinical and/or point of care technique, although samples are usually measured in their dried state [40,41]. Raman spectroscopic analysis of the native liquid samples has been demonstrated to deliver equivalent or improved accuracy, however [42,43]. SERS spectroscopy, using nanoscale noble metal nanostructured substrates or particles can add further sensitivity to the analysis, and functionalisation of the metal surface can be tailored to enhance the molecular specificity of assays [44].

Biosafety is of fundamental concern while working with viruses, as pathogenic agents, and their safe handling is governed by national health and safety legislation, which, for example in the EU is dictated by Directive 2000/54/EC - Biological Agents at Work [45], and subsequent amendments [46], and transposed to national legislation [47]. To simplify how risks from different biological agents are assessed and managed, viruses are categorised into four different risk groups (Groups 1 – 4), based on their ability to cause human disease by infection, and the risk management strategies are associated with Biological Safety Levels (BSL 1-4). Thus, for protection of the individuals handling the virus, and working in the laboratory environment, BSL-2 (Influenza A,B,C, Human respirovirus, Mumps), BSL-3 (Hepatitis B,C, Dengue, SARS) or even BSL-4 (e.g. Ebola) are required [47]. In some cases, risk management by vaccination is additionally advised. All viruses which have already been identified in humans but which have not yet been assessed and classified must be considered to be as group 2 agents at a minimum, unless there is evidence that they are unlikely to be pathogenic to humans.

Routine diagnostic work, through which there is no intention to propagate or concentrate the agents, may be conducted at BSL-2, as can work with specimens that contain or may contain blood-borne viruses. However, additional measures may be required to control the risk of, for example, sharps injuries and contamination of the skin and mucous membranes.

Viruses and virus containing samples can be inactivated for safe handling under normal laboratory conditions (BSL-1) [48], by for example chemical [49,50], heat [51]or radiation treatment [52].

3. Vibrational Spectroscopic analysis of viruses and viral infections:

3.1 Structure and composition of viruses

Although viruses were first described in the late 19th century [53], visualisation of their structures was only possible with the development of electron microscopy in the first half of the 20th [54]. Exploration of the chemical composition of viruses was first facilitated by the isolation of crystallised proteins and nucleic acids from tobacco mosaic viruses [55,56], and by the early 1950s, the chemical constitution of viruses was well described [57]. More recently, the advent of cryo-electron microscopic approaches has enabled near-atomic resolution (2-4 Å) of a wide range of biomolecular

assemblies, including viruses [58,59]. Currently, viruses are classified into families, subfamilies, genus and species, according to their morphology and chemical structure [60]. Electron microscopy remains a key technique for characterising virus morphology [61], while mass spectrometry is extensively utilised to characterise chemical composition [62]. The combination of increasingly sophisticated analytical methods can recreate atomic level models of individual virions, as shown in **Figure 1** for the case of SARS-CoV-2 [63–79].
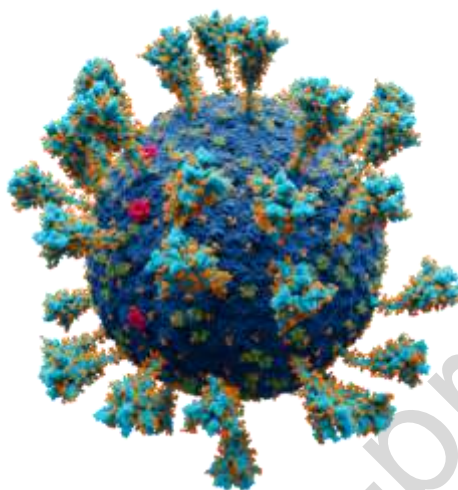
Figure 1: Scientifically accurate atomic model of the external structure of the SARS-CoV-2. Each "ball" is an atom. Colour legend: ▌cobalt - membrane ▌turquoise - spike glycoprotein (S) ▌crimson - E protein ▌green - M protein. ▌orange - glucose (Alexey Solodovnikov (Idea, Producer, CG, Editor), Valeria Arkhipova (Scientific Consultant), CC BY-SA 4.0 <https://creativecommons.org/licenses/by-sa/4.0>, via Wikimedia Commons)

Reports on the use of mid-IR spectroscopy for the direct detection and/or characterisation of viruses are relatively scarce. Vargas *et al*. demonstrated the collection of viral samples form water systems and their measurement by ATR-FTIR [80]. The two viruses, vaccine strain poliovirus type 1 (LSc-2ab) and the bacteriophage MS2, exhibited rich IR spectral profiles, with clear contributions of proteins, lipids and nucleic acids, as well as substantial differences by which they could readily be discriminated. The emerging technique of nano-infrared spectroscopic imaging is of particular interest for the study of viruses. Scanning near-field optical microscopy (s-SNOM) enables (infrared) spectroscopic studies with a spatial resolution as low as 10 nm, allowing high resolution *in situ* spectroscopic chemical and structural identification (**Figure 2**), and the technique was employed to probe structural changes in single enveloped influenza X31virus particles [81]. The study demonstrated the reproducibility of the spectral signatures of individual viral particles, rich in signatures of proteins, lipids and nucleic acids, and was able to monitor the changes in these features in lower pH environments, particularly hemagglutinin, responsible for attachment to the host cell receptor and mediating membrane fusion during virus entry.
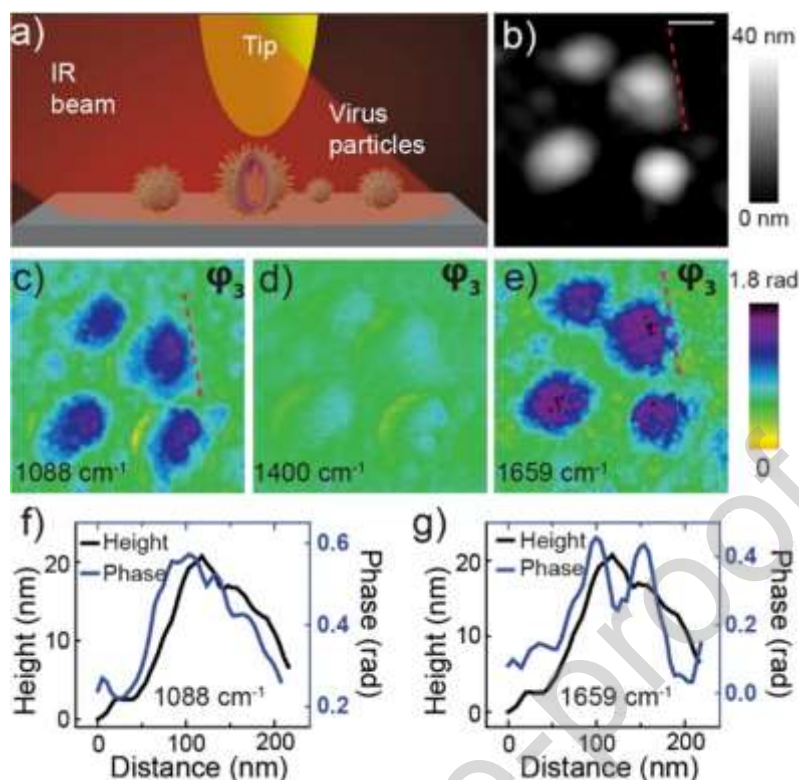
Figure 2: s-SNOM experimental setup and near-field infrared spectral images of influenza virus at pH 7.4. (a) schematic of the s-SNOM experiment, (b) topography of four viruses (scale bar is 100 nm), (c-e) near-field phase (ϕ_3) spectral images at three different frequencies. Line profiles of topography (f) and phase (g) representing the red broken lines shown in the topography (b) and phase (c, e) images. (reproduced from [81] under Creative Commons Licence)

Raman spectroscopic studies of viruses date back to 1978, when Hartman *et al.* undertook an analysis of the turnip yellow mosaic virus (TYMV) [82]. The study examined the secondary structure of the coat-protein and of the encapsulated RNA. Numerous further structural and functional studies followed; of belladonna and bean pod and mottle virus (BPMV) [83–85], Ff filamentous viruses [86,87], the bacteriophages PRD1 and P22 [88,89]. The Raman spectra of purified viruses are rich in information on the constituent lipidic, proteinic, nucleic acid biomolecules and their structures, conformations and organisation, and are an ideal platform to study changes to that structure and organisation. Xu *et al.* undertook a Raman spectroscopic study of the human immunodeficiency virus (HIV) and the effects of hypericin-induced photosensitive damage [90]. Among the more recent studies, Ruokola *et al.* analysed samples of purified Echovirus (EV1), to establish Raman spectroscopic signatures of the virus, and the effects of uncoating using thermal treatment [91].

SERS can be employed for direct spectroscopic characterisation, using non-functionalised nanostructured substrates. In 2001, Bao *et al.* conducted a SERS study of insect nuclear polyhedrosis viruses in silver hydrogels [92], while numerous other studies have used nanostructured metal substrates to study molecular signatures of, for example, respiratory viruses [93,94], rotavirus [95,96] and poxviridae virions [97]. Fan *et al.* demonstrated the use of SERS to detect and discriminate seven food and waterborne viruses in aqueous solution, including noro virus, adeno virus, parvo virus, rota virus, corona virus, paramyxo virus, and herpes virus [98]. Olschewski *et al.* used TERS to detect and discriminate Varicella-zoster virus (VZV) and Porcine teschovirus (PTV) [99]. Viruses were first located in AFM topographic images, after which the TERS profile was mapped according to grids of dimensions varying from 0.05-0.05 μm (12 x 12 points) to 0.40 x 0.40 μm (25 x 25 points) [99]. Differing surface profiles of lipidic and proteinic (VZV), and justproteinic (PTV)

signatures were observed, enabling the development of a linear discriminant analysis (LDA) model with classification accuracy for virus species identification of approximately 91%.

SERS based immunoassays further enhance the specificity of the measurement, by functionalisation of the nanoscale metal surface to bind and measure individual viruses. As an example, Driskell *et al.* used monoclonal antibodies as functional agents for the selective extraction of the feline calicivirus from cell culture media in a chip-scale, sandwich immunoassay, incorporating SERS readout [100]. Effective functionalisation with, for example, specific antibodies [101–103] and glycoproteins [104] has been demonstrated, while the use of oligonucleotides as recognition elements for SERS sensors has recently been reviewed [105]. An alternative approach of size selective capture by gold nanoparticle coated carbon nanotube arrays and detection using SERS has also been demonstrated [106]. The virus capture with detection and identification (VIRRION) platform was initially demonstrated to be able to differentiate between two avian influenza virus subtypes (H5N2 and H7N2) and reovirus, using principal components analysis (PCA) (**Figure 3D**). It was then validated by the successful identification of different viruses in clinical nasopharyngeal swabs from patients who had been diagnosed with rhino-, influenza A, or human parainfluenza type 3 (HPIV 3) virus, with an accuracy of 93%.
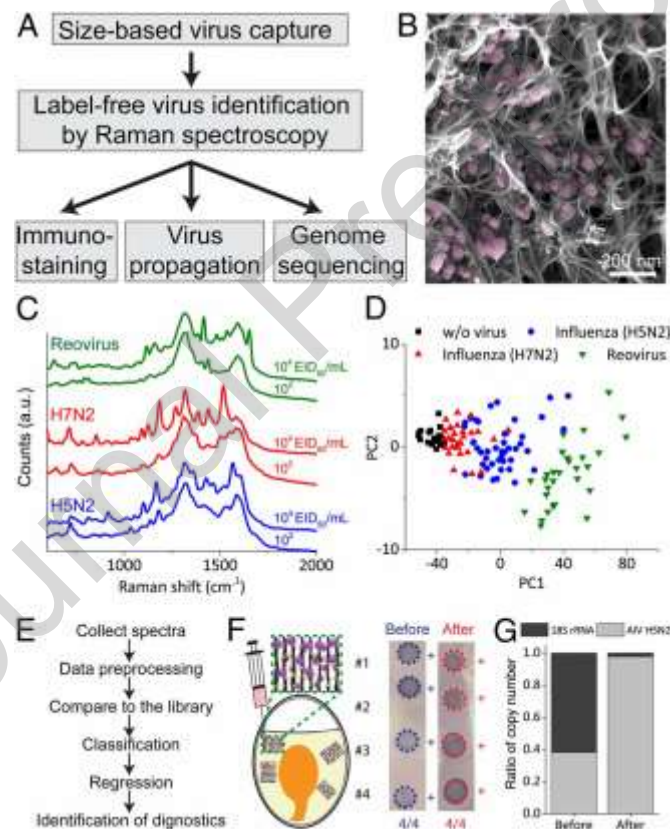
Figure 3: Characterisation of avian influenza virus captured and detected by VIRRION. (A) A process flow of VIRRION for avian influenza virus surveillance and discovery. (B) SEM showing H5N2 virus particles captured by CNxCNT arrays. (C) Raman spectra of H5N2, H7N2, and reovirus collected from VIRRION. (D) Classification by PCA plot of Raman spectra collected from different avian viruses. (E) Process flow of virus identification by Raman spectroscopy with algorithm. (F) H5N2 virus propagated in ECE after viable capture and detection. (G) Ratio of copy number of H5N2 and 18S rRNA before and after VIRRION enrichment. (Reproduced from [106] under Creative Commons Attribution License 4.0 (CC BY))

3.2 Virus Cell Interactions

Viruses employ different mechanisms for host cell invasion and establishment of infections inside the cell. The initial invasion of cells by viruses depends on key interactions between viral envelope proteins and cell surface proteins, the outcome of which determine the efficiency of infection, viral loads and transmission rates [107]. In addition to virus specific receptors, the efficient entry of many viruses into cells depends on interactions with co receptors and accessory cell surface molecules that aid entry and internalisation. The latter interactions can dramatically increase the efficiency of entry by concentrating the virus on the cell surface, thereby increasing the probability of interactions with the fusion receptors. Collectively all these interactions determine pathogenicity, tissue tropism and host range. The identification of host receptors is therefore essential in understanding viral infections and pathogenesis [108]. Various methods like monoclonal antibodies, affinity purification assays and solid phase assays have been extensively exploited in earlier virus-cell interaction studies [109–112]. Advances in techniques like high throughput screening, targeted gene perturbation, mass spectrometry and genetic screening have facilitated the identification of receptors in host cells [113]. These methods are, however, usually based on molecular analyses after cell lysis, and do not visualise the interactions *in situ* [108]. No single method reveals the overall picture of virus entry, and receptors are more commonly identified using a combination of different approaches.

Following membrane penetration, the virus can release its genome into the cytosol or, once again, make use of cellular machinery such as microtubules and their associated motors, to transfer its genome to the nucleus. Replication of the viral DNA or RNA can occur in the cytoplasm or nucleus by transcription followed by translation, after which the virion is reconstructed and released. The rate of viral replication facilitates viral spread whilst evading the host's innate antiviral immune surveillance [114], and viral replication rates have been reported to regulate development of the specific adaptive immune responses in influenza infection [115]. A component of innate immunity to restrict viral replication is the production of cytokines to control the viral infection. However, uncontrolled overproduction of cytokines can lead to the phenomenon of 'cytokine storm', which has been reported in severe COVID-19 patients and influenza infection.

Quantitative polymerase chain reaction is considered to be the principal technique for quantification of viral replication [116,117], and has been employed, for example, to study the regulatory role of microRNAs (miRNAs) in host-virus interactions [118]. The PCR reaction works through amplification and detection of the target gene through a read out process generally based on size and charge, or fluorescence labelling. These techniques involve the use of agarose gels, acrylamide gels, electrophoresis or fluorescent detection of the labelled end product. This well-known molecular technique can be qualitative or qualitative. Real time PCR platforms have been developed to enable detection of RNA within a sample through the mechanism of reverse transcriptase, which transforms RNA into cDNA, known as RT-PCR[119]. Notably, however, as a molecular analysis technique, it does not visualise the virus *in situ*, and does not characterise the infectivity, or host response. In contrast, fluorescence microscopy has been demonstrated to be an effective tool to study virus entry and viral replication inside the host cell, *in situ*. For this purpose, recombinant viruses are generated encoding fluorescent markers, and their expression is monitored as an indicator of viral replication. The technique has been used, for example, to quantify virally infected cells in a monolayer using fluorescence microscopy [120], and to investigate the function of viral proteins and cellular receptors in the process of formation of capsid-nucleus complex [121]. Virus replication can be visualised by using fluorescent probes complementary to the genome of the invading or replicating virus, and fluorescence *in situ* hybridisation (FISH) and confocal microscopy have been employed for the visualisation of the replicating genome [122].

Vibrational spectroscopic techniques offer a more versatile, label free alternative to visualise virus-cell interactions, *in situ*. Although highly sensitive and specific when targeted using surface functionalisation, the SERS effect is limited to a range of ~10nm and so is primarily surface sensitive,

and is limited in its ability to probe virus interactions at a cellular level, to understand mechanisms of membrane penetration, intracellular viral replication, and cellular responses.

Lu *et al.* identified Raman spectroscopic signals associated with conformational changes in the glycoproteins of Nipah virus-like particles (VLPs) [123]. Such conformational changes, as a result of receptor binding, are required for viral entry and cell-cell fusion and the study demonstrated that Raman microspectroscopy can simultaneously identify specific glycoprotein signatures and receptor-induced conformational changes.

Huleihel *et al.* employed FTIR microscopy in transmission mode to spectroscopically profile mouse primary fibroblast and kidney cells, infected with the murine sarcoma virus (MuSV-124) [124]. Both cell types were seen to proliferate much more rapidly once infected, and significant differences were seen in the spectral profiles of the infected cells, potentially associated with phospholipids and nucleic acids, indicative of cell metabolism. Salman *et al.* undertook a similar study to spectroscopically profile normal monkey kidney (Vero), human and rabbit fibroblast cells in culture and cells infected with various members of the herpes family of viruses (Herpes simplex (HSV) and VZV) [125]. Significant spectral differences between normal and infected cells were apparent as early as 24 h post infection, although the morphological differences and indicators of apoptotic onset (caspase 3) were only evident after 3 days. It should be noted, however, that the spectra show potential influences of scattering backgrounds, which may derive from morphological differences [126,127], and therefore interpretation of the spectral differences is not trivial.
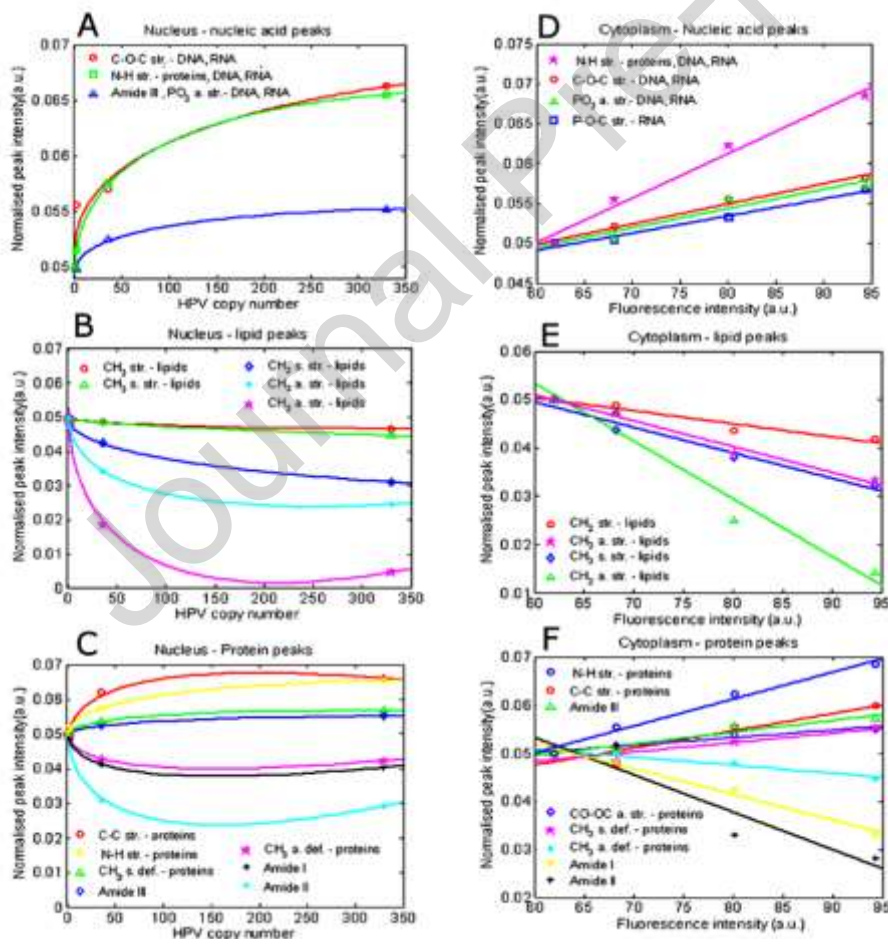
Figure 4: Peak intensity analysis for FTIR spectra of nuclear and cytoplasmic regions of cervical cancer cells. Dependence of peak intensities vs.HPV copy number was fit
with $y = a + b\sqrt{x} + cx$ function, while peak intensities vs. fluorescence intensities (p16^{INK4A} expression level) was fit with a linear function, $y = a + bx$. (Reproduced with permission from [128])

The kinetics of the development of herpes simplex virus (HSV) infection were studied using FTIR microscopy by Erukhimovitch *et al.* [129]. Cultures of Vero cells, infected with HSV types 1 and 2 (HSV-1, HSV-2) and VZV, were monitored spectroscopically over a period of 100 hrs post infection. A change in the cellular shape, from spindle to circular, was observed, as the infection evolves within the cells. Significant increases for infected compared to control cells were observed in the intensities of bands in the region 1200–1400 cm^{-1}, in which the authors identify potential contributions of asymmetric phosphate vibrations at 1235 cm^{-1}. Loss of intensity (1023 cm^{-1}), and continuous shifting (862 cm^{-1}) of bands attributed to carbohydrates were observed only in the infected cells, although there did not appear to be significant differences between the effects of the two viruses. The spectral changes are predominantly ascribed to the increased proliferation of the cells. The spectral regions in which differences are identified are quite broad, however, and alternative band assignments may be more appropriate [130]. A further study of the same system indicated a return of the biochemical profile of infected cells towards that of uninfected at the later stages of infection (24h) [131]. The study of Hastings *et al.* similarly used FTIR microscopy to examine Vero cells infected with HSV-1, as well as human adenovirus type 5 (Ad-5) [132]. Notably, they highlight the potential impact of morphological changes associated with the infection on the spectra recorded, and urge caution in the interpretation of subtle spectral changes. They employed multivariate techniques to demonstrate that it is possible to distinguish infected from uninfected cells, as well as different types of viral infections, with a high degree of accuracy. There have been several reports of IR spectroscopic investigations of human papilloma virus (HPV) infection, particularly relevant for cervical cancer screening [133,134]. Spectra of cell lines infected with different HPV copy number could be well differentiated using multivariate principal components analysis, and a semi-quantitative correlation was drawn between expression of the protein p16 and level of viral infection (**Figure 4**), and a predictive partial least squares regression (PLSR) model was developed, based on the FTIR signatures [128]. Lee- Montiel *et al.* used a similar regression approach to argue that the cell culture itself, monitored by FTIR microscopy, can act as a sensitive and quantitative biosensor for detection of the polio virus [135], while classification models were developed based on ATR-FTIR to classify cervical cytology according to HPV infection [136]. While the limited spatial resolution of the mid-infrared wavelengths (~3-10 μm) restricts the capacity for analysis of biochemical composition at an individual or sub- cellular level, the higher intrinsic resolution of Raman microspectroscopy, commonly performed with visible or near infrared (400-800 nm) sources, more naturally lends itself to such studies. Hamden *et al.* utilised Raman tweezers to examine Kaposi's sarcoma-associated herpes virus (KS-HSV) infected hematopoietic cells (BCBL-1 and BC-1 cells) [137]. PCA indicated that the spectra of the nuclei of infected cells could be differentiated from those of uninfected cells with a high degree of accuracy, largely based on a significant increase in the intensities of bands corresponding to proteins and nucleic acids. Dyson *et al.* demonstrated that Raman tweezers could also differentiate latent and lytic phases of KS-HSV replication, in hematopoietic cells at different stages of infection, sorted by flow cytometry [138]. Salman *et al.* demonstrated the potential of Raman microspectroscopy to differentiate Vero cells infected with HSV-1, achieving ~100% sensitivity [139]. The differentiating spectral features were generically assigned to proteins, lipids and nucleic acids, which were seen to be by reduced in infected cells, it was speculated due to reduced metabolic activity of the lytic virus infected cells. Huleihel *et al.* [140] took a similar approach for the rapid identification of virus infected cells. HSV-1, HSV-2 and VZV were used for the inoculation of Vero cells. Raman spectra of virus infected cell cultures were then classified using PCA-LDA, achieving 97% classification accuracy. Odintsova *et al.* employed Raman microspectroscopy to identify herpes-like virus infection in haemocytes of the red king crab *Paralithodes camtschaticus* [141], characterised by a change in pigmentation, associated with strong melanin features in the 532nm Raman spectra of the cells. Although limited in spatial sensitivity, Lim *et al.* demonstrated that SERS could be employed to differentiate between different emerging influenza virus strains based on the analysis of infected Human embryonic kidney (HEK) 293T cells [142].

A number of studies have employed Raman microspectroscopy in a time lapse fashion to monitor the evolution of viral infection, at a cellular level. Moor *et al.* used Raman microspectroscopy to detect adenovirus infection in live HEK 293 cells and to monitor the evolution of the nuclear spectra at 12, 24,and 48 h after initiation of the infection [143]. Infected cells were clearly differentiated from non-infected, based on their spectroscopic profiles, although the temporal evolution of the spectral features was not well elucidated. In a further study, Moor *et al.* demonstrated that Raman microspectroscopy could detect adenovirus virus infection in live HEK 293 cells within 3 h of invagination [144]. The Raman signatures were monitored at 3, 6, 9, 12, 18, and 24 h, showing a clearer evolution of the spectral features. A significant change was seen between 6 and 9 hrs, indicating an abrupt reduction in the proteinic content of infected cells. Pezzotti *et al.* monitored the evolution of Influenza A virus infection in a model Madin–Darby canine kidney (MDCK) cell line [145]. Spectra (using 532 nm s source) were recorded from the live MDCK cells as well as of the virus, and of the inoculated cells after 48 and 72 hr. The spectral profiles at the later stages of evolution could not be described by a simple weighted sum of the cellular and virus spectral profiles. Deconvolution of the spectral profiles using Gaussian-Lorentzian bands enabled tracking of the evolution of specific features associated with the metabolic evolution of the cell and virus. The evolution was seen to be consistent, for example, with an increase in viral RNA at the expense of host cellular DNA replication, and indicated important roles of glucose and lipidic components in the replication process. The study of Tiwari *et al.* [146] monitored the temporal evolution (2, 4, 6, 12, 24, 36, and 48 h) of the Raman microspectroscopic signatures associated with the replication of Epstein–Barr virus Infection in the nuclei and peripheral regions of human glial cells, HMC-3 (microglia) and U-87 MG (astrocytes). Spectral features of, amongst others, cholesterol ($548 cm^{-1}$), glucose ($540, 117 cm^{-1}$), the amino acids phenylalanine, tyrosine and tryptophan ($1600–1628 cm^{-1}$) and phosphatidylinositol ($776 cm^{-1}$) are identified, associated by the authors with cellular processes such as lipid transport, cell proliferation, differentiation, and apoptosis in the cells. A pathway analysis of selected biomolecules was undertaken, projecting potential links with systemic responses to viral infection, including neuropathologies such as Alzheimer's disease and multiple sclerosis.

3.3 Monitoring viral infection

The current, clinically approved, gold standard for screening and identification of viral infections is reverse transcription polymerase chain reaction (RT-PCR), which directly measures and quantifies the viral DNA/RNA [147,148]. As a screening test, it has high sensitivity, high specificity, and is inherently quantitative in nature. However, as a molecular test, it requires significant processing to extract, amplify and detect the relevant nucleic acid sample, making it relatively time consuming, laborious and costly. Recent events have demonstrated that the development of rapid, field deployable, automated, cost effective and reliable screening methods for viruses is paramount in the fight against disease. This is crucial to enable monitoring of disease outbreaks, and patient prognosis and treatment. Analysis of the viral load and systemic biochemical responses is also vital for monitoring disease progression and the impacts of therapeutic interventions [3,149].

As an alternative to PCR testing, antigen tests are cheap and rapid in comparison, they can be self administered, and results may be obtained within 15 minutes of the sample being acquired. This chromatographic immunoassay detects specific antigens directed against the specified virus. Although a recent study has estimated that the lateral flow antigen test for SARS-CoV-2 has an 83-91% accuracy for detection of positive samples [150], it is less sensitive than the gold standard PCR test and can fail to identify infection in individuals with a lower viral load [151].

Serological antibody testing may be carried out to determine whether an individual has contracted an infection in the recent past, or to monitor the systemic response to viral infection. If an individual is infected with a virus, the body's immune system will recognise viral antigens such as the spike protein and nucleocapsid protein and thus initiate an immune response [152]. This response triggers T-cell activation and leads to virus specific immunoglobulin (Ig) antibody production. Antibodies are reportedly detectable in the blood serum days after initial infection, but begin to fade during

convalescence on a varied timescale of weeks to months [149,153,154]. Differential analysis of antibodies can be an important aspect of diagnosis, as, for example, acute, early stage infection can be confirmed by the presence of IgM (immunoglobulin M), whereas elevated IgG levels can indicate late stage or previous infection [155,156]. Antibody tests are based on ELISA, chemiluminescent immunoassays and other techniques and, although useful for epidemiological studies and also healthcare workers, are not recommended as a diagnostic test for acute infections.

The potential of spectroscopic analysis to detect the presence of blood borne viral infection has been extensively explored. In blood based analysis, very notable and eye-catching translational work by the group from Monash University, based on the use of ATR –FTIR spectroscopy for the determination of malaria parasitemia in whole blood samples, has been recently demonstrated in field trials in austere environments, proving the robustness and capability of serum biofluid [12]. Roy *et al.* also demonstrated the use of the technique for the detection of HBV and HCV infection in human serum [157]. The sensitivity and specificity of the technique was seen to be significantly enhanced by fractionation of the serum samples into high and low molecular weight components. Using Partial Least Squares-Discriminative Analysis (PLS-DA), sensitivities and specificities of 87.5 % and 94.9 %, respectively for HBV vs control, and 81.6 % and 89.6 %, respectively for HCV vs control were achieved, in both cases for the high molecular weight fractions. Another example of the practicality of ATR-FTIR as a diagnostic tool for viruses in human bodily fluids was demonstrated by the detection of HIV in the study conducted by Silva et al. [158]. Based on a patient cohort of 40 HIV positive pregnant women and 80 uninfected controls, they received a classification accuracy of 89% using a DA algorithm. In another study, it was shown how FTIR can detect HPV in cervical fluid samples with a classification of 100% efficiency within the spectral ranges 1400-1800 cm^{-1} [159] and furthermore could differentiate between low risk HPV and high risk HPV with 71-75% efficiency. ATR-FTIR has thus proven to be a very useful method for viral diagnosis, not only is it rapid and cost effective technique and coupled with only a minuscule amount of body fluid is needed for accurate results, making this method a good candidate to translate to the clinical benchtop [33].

The advantages of Raman spectroscopic screening of liquid serum samples over IR screening of dried serum samples have recently been demonstrated for the case of glucose monitoring [42]. Saade *et al.* [14], demonstrated the potential of Raman spectroscopic analysis of liquid sera samples to discriminate between normal and HCV patient samples. Ditta *et al.* [160] used a similar approach to differentiate spectral markers of low, medium and high HCV loads. Saleem *et al.* [161] reported a Raman spectroscopic analysis of dengue virus infection in (dried) human blood serum samples using Raman spectroscopy, and although a PLSR model was constructed, with a reported root mean squared error (RMSE) of prediction of 0.0099 and correlation coefficient (R^2) of 0.9998, it was based only on normal/infected, rather than a continuous variation of viral load. Khan *et al.* [162] used Raman spectroscopy, coupled with support vector machine analysis, to diagnose dengue infection based on positive IgM status, in samples of human serum dried on glass slides, with a high degree of accuracy (85%) and precision (90%), and corresponding sensitivity and specificity of 73% and 93%, respectively.

In a more quantitative approach, Bilal *et al.* [163] performed a Raman spectroscopic analysis of dengue infected human serum samples in liquid form, and, based on PLSR analysis of data of IgM positive and normal human serum samples, established a prediction model with a correlation co-efficient R^2 of 0.929 and RMSE of cross validation for the entire predicted values of ~10%. Using the receiver operating characteristic curve (ROC) approach, an accuracy of 96.67%, a sensitivity of 90% and a specificity of 100% were reported. In a similar approach, using Raman spectroscopy coupled with PLSR analysis, Nawaz *et al.* [164] reported a RMSE of prediction of 0.2%, for HCV load in liquid samples of human blood plasma, as measured by the current clinical gold standard, PCR. Although the study was only performed on a patient cohort of 10, and the methodology optimisation not explored extensively, the result justifies further exploration of the technique for clinical translation.

It is notable, however, that in the analysis of blood serum, no signatures of the virus itself have been unambiguously identified. However, El-Said and Choi developed a spectroelectrochemical biosensor to detect the RNA extracted from human serum of HCV positive patients [165]. Immobilising a specific peptide nucleic acid on a gold nanoparticle surface as a highly selective bio-receptor, Raman spectroscopy and Square wave voltammetry was employed for the detection of HCV – RNA with a sensitivity of ~ 1×10^3 IU/mL. Furthermore, Batool *et al.* used a non selective SERS approach to measure the PCR extracted DNA products from the blood serum of HBV positive patients [166], and Nasir et al. used a similar methodology for analysis of the blood of HCV positive patients [167].

More generally, spectroscopic analysis of bodily fluids, particularly blood, have registered the systemic response to infection by viruses, both blood borne and otherwise. The most prominent of these is the immunoglobulin response, as indicated by Roy *et al.* [157], correlation with which was used to build a quantitative model for prediction of HCV load by Nawaz *et al.* [164].

4. SARS-CoV-2 and COVID 19: Contributions to date and Future perspectives

The potential role of spectroscopy in the global response to the COVID-19 pandemic has been discussed extensively [168–171]. A range of different potential applications have been considered, in environmental and patient screening for the presence of SARS-CoV-2, clinical diagnosis of COVID 19, and long term monitoring of convalescing patients and the effects of vaccination. Previous studies have demonstrated that the techniques are rapid, relatively non-invasive, require minimal sample preparation, and are field deployable [12,172].

It has been demonstrated that SERS can be employed for the detection of the SARS-CoV-2 virus in environmental samples, using a silver-nanorod SERS array functionalised with the cellular receptor angiotensin-converting enzyme 2 (ACE-2) [173]. The developed ACE2@SN-SERS assay provides good accuracy and satisfactory performance for the rapid and onsite diagnosis of SARS-CoV-2 in environmental specimens from rivers, hospitals and pipe networks in Wuhan (China), consistent with the results of Quantitative reverse transcription PCR (RT-qPCR [174]). Compared with RT-qPCR and ELISA assays, this ACE2@SN-SERS assay has three advantages, as (1) it does not rely on RNA extraction or immune biomarker, simplifying the sample preparation procedure and shortening the measurement time, (2) the spike protein is more stable than RNA as the biomarker for SARS-CoV-2, suggesting a more stable and sensitive assay particularly, for environmental specimens, (3) it was demonstrated that portable Raman spectrometers can provide satisfactory signals with the ACE2@SN-SERS assay, potentially enabling rapid and specific interrogation of SARS-CoV-2 on site.

More recently, Wood *et al.* purified SARS-CoV-2 virion particles from the supernatant of Vero cells, deactivated them by fixation with 4 % formalin, and characterised them using Raman, synchrotron IR and AFM-IR spectroscopies (**Figure 5**) [175]. The ~120nm in diameter virus particles exhibited characteristic spectral features of spike, envelope, membrane and nucleocapsid proteins (1657, 1547, 1517 cm^{-1}), lipids of the bilayer surrounding the nucleocapsid (1740, 1464, 1382 and 1341 cm^{-1}) and multiple bands associated with RNA in both IR (1690, 1235, 1124, 1089, 996, 967 and 934 cm^{-1}) and Raman (1242, 1110, 807, 782, 723 and 670 cm^{-1}) spectra.

In terms of clinical applications, Schorer et al. explored the use of ATR-IR for diagnosis of infection in a direct face mask sampling approach, differentiating water, proteins, and virus-like particles sampled on the mask [176]. On the basis of their characteristic spectral signatures, Barauna *et al.* argued the potential to establish COVID-19 positivity in human saliva samples using IR spectroscopic screening [177]. Using saliva samples spiked with inactivated COVID-19 virus particles, they demonstrated that, for low copy numbers, the IR spectral signature of the spiked saliva could be differentiated by discriminating features primarily associated with RNA. Analysis of pharyngeal swabs from patients (*n*= 111 negative and 70 positive) by ATR-IR indicated that a diagnostic sensitivity of 95% and specificity of 89% could be achieved, based on a genetic algorithm-discriminant analysis. A further study conducted by Nogueira *et al.* sought to verify the use of ATR FTIR as a potential method for screening for SARS-CoV-2 infection. Utilising oropharyngeal swabs of

243 individuals coupled with PLS-DA, it was shown to have an 84-87% sensitivity and 64-66% specificity, when compared to the standard PCR method [178], somewhat lower than the results reported by Barauna *et al.* [177]. Wood *et al.* followed an alternative route of optimising the sampling geometry for improved signal to noise ratio compared to ATR-IR, to demonstrate the potential of transflection based IR spectroscopy for rapid point-of-care detection of SARS-CoV-2 markers in saliva. Based on a patient cohort of 29 positive and 28 negative for SARS-CoV-2 by RT-qPCR, diagnostic sensitivities and specificities of 93 % and 82 %, respectively were achieved. Notably, although the diagnostic performances are comparable, the authors have commented on the validity of the results obtained by Barauna *et al.* [177,179]. Nevertheless, the studies demonstrate the potential of ATR-IR as an efficient, field deployable method for populations screening for SARS-CoV-2 infection. In a follow up study, Kazmer et al. undertook a study to examine the pathophysiological response underpinning the differentiating IR spectroscopy signature of SARS-CoV-2 infection [180]. FTIR studies of the supernatant of Vero E6 cells in vitro and oral lavage samples of K18-hACE2 mice which had been treated with active of UV-inactivated SARS-CoV-2, indicated that booth treatments resulted in spectroscopic signatures which were different to untreated controls, although the active virus treatment resulted in specific spectral changes to the amide I/II bands (1700–1470 cm^{-1}) and fingerprint region (1450–600 cm^{-1}), notably the symmetric stretching of phosphodiester linkages of RNA (vsPO2−) at 1124 cm^{-1}, which were attributed to aggregated proteins and RNA. A predictive model for COVID-19 using PLS-DA based on spectroscopic analysis of saliva from a cohort of human participants (n= 104) produced a sensitivity of 93.48%, and it was noted that COVID-19 vaccination did not lead to the misclassification of COVID-19 negatives. A meta-analysis of the results of the study, and other cohort studies indicated that altered beta-sheet structures in secreted proteins, resulting in changes in the amide II band may be considered a spectral marker for SARS-CoV-2 infection.
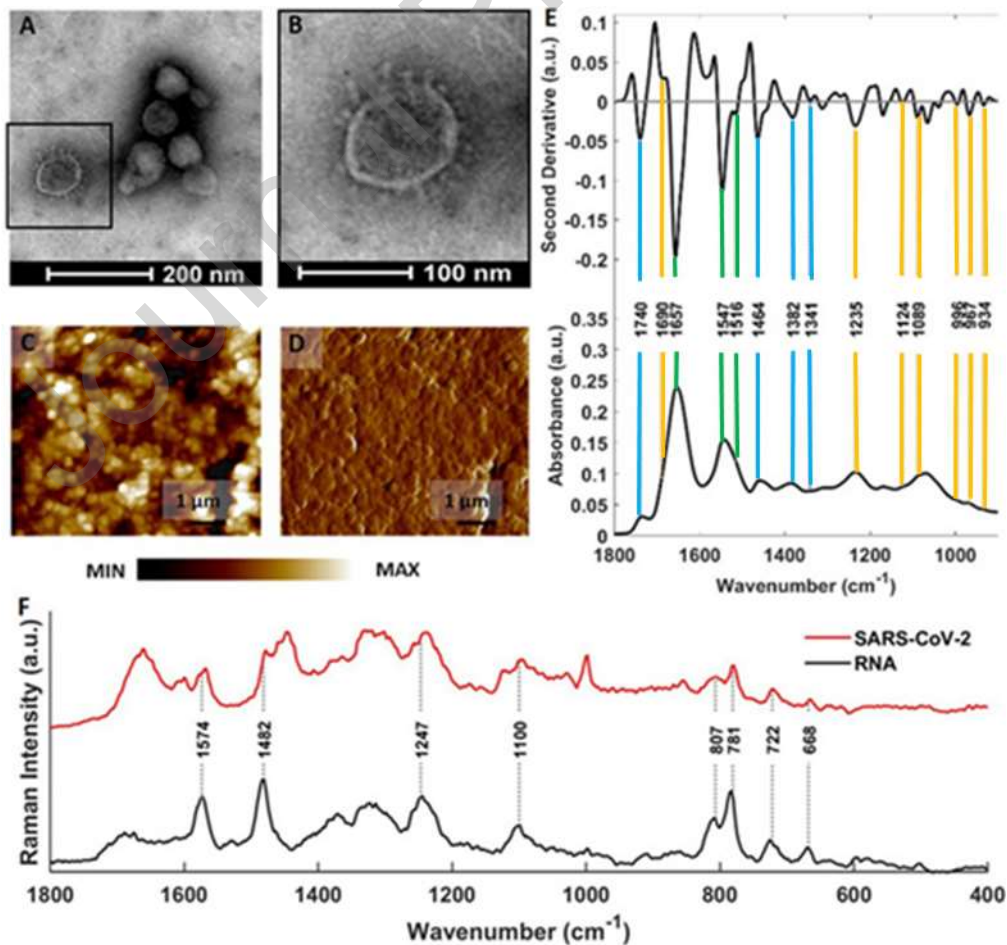
Figure 5: AFM, TEM, synchrotron FTIR and Raman characterization of SARS-CoV-2 virus. A–E) A) TEM image of SARS-CoV-2 sample with single virion marked by black square. B) Magnification of the area marked by the black square in (A), showing a single SARS-CoV-2 particle with its characteristic morphological appearance. C) AFM height and D) AFM deflection images of SARS-CoV-2 sample, demonstrating multiple round structures. E) Synchrotron FTIR spectrum and its 2nd derivative transform with the most prominent bands marked. The bands are color-coded as follows: lipids (blue), proteins (green) and nucleic acids (orange). F) Raman spectrum (532 nm) of SARS-CoV-2 virions (red) compared to spectrum of purified RNA (black) with labelled bands. (Reproduced with permission from [175])

Zhang *et al.* conducted a study of dried human blood serum samples to show that ATR-FTIR can be used as a clinical diagnostic tool for COVID-19 [181]. In the study of 20 healthy donors and 76 patients, including 41 which were confirmed COVID-19 positive, 15 which had respiratory viral infections caused by influenza A/B or respiratory syncytial virus (RSV), and 20 which had inflammation-related diseases, they found that the FTIR method was able to distinguish between other common respiratory viruses versus COVID-19 with a specificity of 98% and sensitivity of 83.1%.

Yin *et al.* have recently presented a Raman spectroscopic study of 177 blood serum samples, collected from 63 confirmed COVID-19 patients, 59 suspected cases, and 55 healthy individuals, reporting a classification accuracy of 87% for COVID-19 positive versus the suspected cases, and an accuracy of 90% for the COVID-19 positive cases and the healthy controls [182]. For the measurement, ~0.5 ml of the serum was sealed in polypropylene cryopreservation tubes, to minimise exposure. However, the spectrum of the polypropylene itself contributes significantly to the measured serum spectrum. Although there has been no direct comparison of Raman and ATR-FTIR techniques for monitoring COVID-19 in blood, studies of glucose in blood serum have indicated comparable accuracies of the techniques [42] and the requirement for sample drying for ATR-FTIR may favour the use of Raman analysis of liquid serum samples for COVID-19 monitoring [40]. More recent studies have demonstrated the efficacy of a silver nanoparticle based SERS assay to detect, spectrally characterise and differentiate the viruses SARS-CoV-2, human adenovirus 3, and H1N1 influenza virus at a concentration of 100 copies/test (PFU/test) in PBS, or spiked in human serum of saliva [183].

IR absorption and Raman spectroscopies have therefore been demonstrated to hold significant potential for high sensitivity/specificity, rapid, field deployable screening technologies, as well as clinical diagnostic techniques. Notably, in this context, it has been reported that, although low levels of SARS-CoV-2 RNA have been detected in the serum of COVID-19 patients, they are not associated with infectious virus, suggesting that reduced biosafety precautions are required for investigations of blood samples of COVID-19 positive or previously positive patients [184]. Pending the availability of samples, of particular interest would be longitudinal studies of patient responses, which may support a better understanding of the recovery and convalescence process, long term effects of COVID, immune responses and vaccine efficacies. As an example, the FTIR microspectroscopic study of Bandeira et al. analysed dried serum samples from healthy and COVID-19 positive individuals, exhibiting mild or more severe symptoms indicated that the carbonyl C=O vibration (1702–1785 cm^{-1}) is a spectral marker of the degree of IgG glycosylation, enabling the classification of sub-populations of COVID-19 patients, depending on the degree of disease severity [185].

Understanding the process of viral attachment to, entry into, replication within, and release from cells is a critical aspect of infection control, understanding the mechanism of action of emerging viruses, and monitoring their mutation to new strains. The requirements for Biological Safety Level 3 (BCL-3) laboratory conditions has largely precluded the *in situ* study of SARS-CoV-2 attachment to, invasion of and replication in cells, although Akdeniz et al. have recently developed a virus-infected HEK293 cell model, transfected with plasmids encoding the nucleocapsid, membrane and envelope proteins of SARS-CoV-2 [186]. Gold nanoparticle SERS combined with PCA identified largely protein

markers which differentiated transfected and nontransfected cells although the process of transfection was not explicitly studied. In this context, pseudoviruses have been demonstrated to be useful to study viral attachment and cellular entry processes, as well as antibody neutralisation assays [187], or simply viral detection strategies [188]. Such pseudoviruses are relatively easily generated using retro/lentivirus templates [189], and can be tailored to express different surface spike protein configurations to mimic and study the behaviours of emerging mutations. Fluorescence labelling is often employed to monitor the attachment and entry processes under BCL-2 conditions, but *in situ*, label free vibrational spectroscopic analysis could provide a more holistic picture of the processes. Raman microspectroscopy lends itself more naturally to such analysis of processes in live cells [190], and, although they do not facilitate the study of the replication process, pseudovirus studies can contribute to the development of the microspectroscopic methodology, and particularly data mining approaches. The study of non- or mildly pathogenic viruses, such as the murine respirovirus (Sendai) [191], or the circulating human CoV-NL63 strain [192], can be similarly employed to study viral replication processes in cells, towards optimisation of the methods.

An aspect of virology which has not yet been explored by spectroscopy is that of the viral release process. Enveloped viruses are typically secreted from the host cell by budding. It is this process that results in the acquisition of the viral phospholipid envelope. In the process, the cell can also secrete numerous other species, such as molecular cytokines, which can also be enveloped in lipidic vesicles. The role of extracellular particles in viral infection and responses has been discussed [193,194], and released virus particles have even been considered as exosomes [195]. Limited spectroscopic studies have been undertaken to address the release of viral particles and other factors from cells, although vibrational spectroscopy has been successfully employed to characterise exosomes and extracellular vesicles in a number of biological systems [196–198]. Raman spectroscopy was used to study the chemical composition of single exosomes from 8 cell lines [199], and a high degree of variance was seen between the mean spectral signatures of the cell lines, as well as individual exosomes from the same cell type. The results indicated that the spectral signatures represented characteristic and distinct exosomal protein, lipid, genetic, and cytosolic content, reflecting the cellular response mechanism, and could be employed to differentiate cancer from non-cancer cells based on their relative expression of cholesterol and phospholipids. While the higher spatial resolution of Raman microspectroscopy approaches the dimensions of exosomes, and Raman tweezers measurements have been shown to be capable of addressing individual particles [200], IR spectroscopy has been demonstrated to be effective in characterising separated populations of exosomes, for which Amide and C H stretching band intensity ratios calculated from IR bands, characteristic of protein and lipid components, proved to be distinctive for the different extracellular vesicle subpopulations [201]. Spectropscopic anlysis of purified exosomal samples extracted at different timepoints of the life cycle of the virus, using infrared absorption and/or Raman microspectroscopy may therefore add considerably to the understanding of the processes, and the contributions of the techniques to the field.

Acknowledgements

References

[1]   S. Singh, A battle between viruses and humans: Who is the winner?, Int. J. Clin. Pract. 75 (2021) 3–4. https://doi.org/10.1111/ijcp.13903.

[2]   N. Nandal, G. Uma, The Epidemics and Pandemics in the world : A study, IX (2020) 194–197.

[3]   World Health Organization, A coordinated Global Research Roadmap to respond to theD-19 epidemic and beyond, 2020.

[4]   N.M. Ralbovsky, I.K. Lednev, Towards development of a novel universal medical diagnostic method: Raman spectroscopy and machine learning, Chem. Soc. Rev. 49 (2020) 7428–7453. https://doi.org/10.1039/d0cs01019g.

[5]   M.J. Baker, H.J. Byrne, J. Chalmers, P. Gardner, R. Goodacre, A. Henderson, S.G. Kazarian, F.L. Martin, J. Moger, N. Stone, J. Sulé-Suso, Clinical applications of infrared and Raman spectroscopy: State of play and future challenges, Analyst. 143 (2018) 1735–1757. https://doi.org/10.1039/c7an01871a.

[6]   H.J. Byrne, M. Baranska, G.J. Puppels, N. Stone, B. Wood, K.M. Gough, P. Lasch, P. Heraud, J. Sulé-Suso, G.D. Sockalingum, Spectropathology for the next generation: Quo vadis?, Analyst. 140 (2015) 2066–2073. https://doi.org/10.1039/c4an02036g.

[7]   H.J. Byrne, G.D. Sockalingum, N. Stone, Raman microscopy: Complement or competitor?, in: D. Moss (Ed.), RSC Anal. Spectrosc. Ser., RSC Analytical Spectroscopy Series, 2011: pp. 105–143. https://doi.org/10.1039/9781849731997-00105.

[8]   H.J. Byrne, F. Bonnier, A. Casey, M. Maher, J. McIntyre, E. Efeoglu, Z. Farhane, Advancing Raman microspectroscopy for cellular and subcellular analysis: towards in vitro high-content spectralomic analysis, Appl. Opt. 57 (2018) E11. https://doi.org/10.1364/ao.57.000e11.

[9]   Z. Farhane, F. Bonnier, A. Casey, H.J. Byrne, Raman micro spectroscopy for in vitro drug screening: Subcellular localisation and interactions of doxorubicin, Analyst. 140 (2015) 4212–4223. https://doi.org/10.1039/c5an00256g.

[10]   K. Naseer, S. Ali, J. Qazi, ATR-FTIR spectroscopy as the future of diagnostics: a systematic review of the approach using bio-fluids, Appl. Spectrosc. Rev. 56 (2021) 85–97. https://doi.org/10.1080/05704928.2020.1738453.

[11]   E. Barnas, J. Skret-Magierlo, A. Skret, E. Kaznowska, J. Depciuch, K. Szmuc, K. Łach, I. Krawczyk-Marć, J. Cebulski, Simultaneous ftir and raman spectroscopy in endometrial atypical hyperplasia and cancer, Int. J. Mol. Sci. 21 (2020) 1–13. https://doi.org/10.3390/ijms21144828.

[12]   S. Roy, D. Perez-Guaita, D.W. Andrew, J.S. Richards, D. McNaughton, P. Heraud, B.R. Wood, Simultaneous ATR-FTIR Based Determination of Malaria Parasitemia, Glucose and Urea in Whole Blood Dried onto a Glass Slide, Anal. Chem. 89 (2017) 5238–5245. https://doi.org/10.1021/acs.analchem.6b04578.

[13]   M. Sbroscia, M. Di Gioacchino, P. Ascenzi, P. Crucitti, A. di Masi, I. Giovannoni, F. Longo, D. Mariotti, A.M. Naciu, A. Palermo, C. Taffon, M. Verri, A. Sodo, A. Crescenzi, M.A. Ricci, Thyroid cancer diagnosis by Raman spectroscopy, Sci. Rep. 10 (2020) 1–10. https://doi.org/10.1038/s41598-020-70165-0.

[14]   J. Saade, M.T.T. Pacheco, M.R. Rodrigues, L. Silveira, Identification of hepatitis C in human blood serum by near-infrared Raman spectroscopy, Spectroscopy. 22 (2008) 387–395. https://doi.org/10.3233/SPE-2008-0344.

[15]   I. Setyopranoto, Role of oxidative stress on acute ischaemic stroke, J. Kedokt. Dan Kesehat. Indones. 7 (2009) 151–160. https://doi.org/10.20885/jkki.vol7.iss4.art6.

[16]   H.J. Byrne, F. Bonnier, J. McIntyre, D.R. Parachalil, Quantitative analysis of human blood serum using vibrational spectroscopy, Clin. Spectrosc. 2 (2020) 100004. https://doi.org/10.1016/j.clispe.2020.100004.

[17]   D.R. Parachalil, J. McIntyre, H.J. Byrne, Potential of Raman spectroscopy for the analysis of plasma/serum in the liquid state: recent advances, Anal. Bioanal. Chem. 412 (2020) 1993–

2007. https://doi.org/10.1007/s00216-019-02349-1.

[18]   S. Wartewig, Basic Principles of Vibrational Spectroscopy, in: IR Raman Spectrosc., John Wiley & Sons, Ltd, 2004: pp. 27–33. https://doi.org/10.1002/3527601635.ch4.

[19]   M.J. Tobin, L. Puskar, R.L. Barber, E.C. Harvey, P. Heraud, B.R. Wood, K.R. Bambery, C.T. Dillon, K.L. Munro, FTIR spectroscopy of single live cells in aqueous media by synchrotron IR microscopy using microfabricated sample holders, Vib. Spectrosc. 53 (2010) 34–38. https://doi.org/10.1016/j.vibspec.2010.02.005.

[20]   K. Isensee, N. Kröger-Lui, W. Petrich, Biomedical applications of mid-infrared quantum cascade lasers-a review, Analyst. 143 (2018) 5888–5911. https://doi.org/10.1039/c8an01306c.

[21]   A. Dazzi, C. Policar, AFM-IR: Photothermal infrared nanospectroscopy: Application to cellular imaging, in: Biointerface Charact. by Adv. IR Spectrosc., Elsevier, 2011: pp. 245–278. https://doi.org/10.1016/B978-0-444-53558-0.00009-6.

[22]   K. Kanevche, D.J. Burr, D.J. Nürnberg, P.K. Hass, A. Elsaesser, J. Heberle, Infrared nanoscopy and tomography of intracellular structures, Commun. Biol. 4 (2021) 1–8. https://doi.org/10.1038/s42003-021-02876-7.

[23]   E. Efeoglu, M.A. Maher, A. Casey, H.J. Byrne, Toxicological assessment of nanomaterials: the role of in vitro Raman microspectroscopic analysis, Anal. Bioanal. Chem. 410 (2018) 1631–1646. https://doi.org/10.1007/s00216-017-0812-x.

[24]   H.J. Byrne, F. Bonnier, E. Efeoglu, C. Moore, J. McIntyre, In vitro Label Free Raman Microspectroscopic Analysis to Monitor the Uptake, Fate and Impacts of Nanoparticle Based Materials, Front. Bioeng. Biotechnol. 8 (2020). https://doi.org/10.3389/fbioe.2020.544311.

[25]   Z. Farhane, H. Nawaz, F. Bonnier, H.J. Byrne, In vitro label-free screening of chemotherapeutic drugs using Raman microspectroscopy: Towards a new paradigm of spectralomics, J. Biophotonics. 11 (2018). https://doi.org/10.1002/jbio.201700258.

[26]   N. Kumar, B.M. Weckhuysen, A.J. Wain, A.J. Pollard, Nanoscale chemical imaging using tip-enhanced Raman spectroscopy, Nat. Protoc. 14 (2019) 1169–1193. https://doi.org/10.1038/s41596-019-0132-z.

[27]   A. Bonifacio, S. Cervo, V. Sergo, Label-free surface-enhanced Raman spectroscopy of biofluids: Fundamental aspects and diagnostic applications, Anal. Bioanal. Chem. 407 (2015) 8265–8277. https://doi.org/10.1007/s00216-015-8697-z.

[28]   A. Campion, P. Kambhampati, Surface-enhanced Raman scattering, Chem. Soc. Rev. 27 (1998) 241–250. https://doi.org/10.1039/a827241z.

[29]   M.J. Baker, S.R. Hussain, L. Lovergne, V. Untereiner, C. Hughes, R.A. Lukaszewski, G. Thiéfin, G.D. Sockalingum, Developing and understanding biofluid vibrational spectroscopy: A critical review, Chem. Soc. Rev. 45 (2016) 1803–1818. https://doi.org/10.1039/c5cs00585j.

[30]   L.B. Leal, M.S. Nogueira, R.A. Canevari, L.F.C.S. Carvalho, Vibration spectroscopy and body biofluids: Literature review for clinical applications, Photodiagnosis Photodyn. Ther. 24 (2018) 237–244. https://doi.org/10.1016/j.pdpdt.2018.09.008.

[31]   A.L. Mitchell, K.B. Gajjar, G. Theophilou, F.L. Martin, P.L. Martin-Hirsch, Vibrational spectroscopy of biofluids for disease screening or diagnosis: Translation from the laboratory to a clinical setting, J. Biophotonics. 7 (2014) 153–165. https://doi.org/10.1002/jbio.201400018.

[32] A.A. Bunaciu, Ş. Fleschin, V.D. Hoang, H.Y. Aboul-Enein, Vibrational Spectroscopy in Body Fluids Analysis, Crit. Rev. Anal. Chem. 47 (2017) 67–75. https://doi.org/10.1080/10408347.2016.1209104.

[33] A. Sala, D.J. Anderson, P.M. Brennan, H.J. Butler, J.M. Cameron, M.D. Jenkinson, C. Rinaldi, A.G. Theakstone, M.J. Baker, Biofluid diagnostics by FTIR spectroscopy: A platform technology for cancer detection, Cancer Lett. 477 (2020) 122–130. https://doi.org/10.1016/j.canlet.2020.02.020.

[34] K. Gajjar, J. Trevisan, G. Owens, P.J. Keating, N.J. Wood, H.F. Stringfellow, P.L. Martin-Hirsch, F.L. Martin, Fourier-transform infrared spectroscopy coupled with a classification machine for the analysis of blood plasma or serum: A novel diagnostic approach for ovarian cancer, Analyst. 138 (2013) 3917–3926. https://doi.org/10.1039/c3an36654e.

[35] S. Derruau, C. Gobinet, A. Mateu, V. Untereiner, S. Lorimier, O. Piot, Shedding light on confounding factors likely to affect salivary infrared biosignatures, Anal. Bioanal. Chem. 411 (2019) 2283–2290. https://doi.org/10.1007/s00216-019-01669-6.

[36] J.J.W. Mikkonen, J. Raittila, L. Rieppo, R. Lappalainen, A.M. Kullaa, S. Myllymaa, Fourier transform infrared spectroscopy and photoacoustic spectroscopy for saliva analysis, Appl. Spectrosc. 70 (2016) 1502–1510. https://doi.org/10.1177/0003702816654149.

[37] S. Gonchukov, A. Sukhinina, D. Bakhmutov, S. Minaeva, Raman spectroscopy of saliva as a perspective method for periodontitis diagnostics, Laser Phys. Lett. 9 (2012) 73–77. https://doi.org/10.1002/lapl.201110095.

[38] G. Calado, I. Behl, A. Daniel, H.J. Byrne, F.M. Lyng, Raman spectroscopic analysis of saliva for the diagnosis of oral cancer: A systematic review, Transl. Biophotonics. 1 (2019) e201900001. https://doi.org/10.1002/tbio.201900001.

[39] G. Calado, I. Behl, H.J. Byrne, F.M. Lyng, Raman spectroscopic characterisation of non stimulated and stimulated human whole saliva, Clin. Spectrosc. 3 (2021) 100010. https://doi.org/10.1016/j.clispe.2021.100010.

[40] J.M. Cameron, H.J. Butler, D.S. Palmer, M.J. Baker, Biofluid spectroscopic disease diagnostics: A review on the processes and spectral impact of drying, J. Biophotonics. 11 (2018) 1–12. https://doi.org/10.1002/jbio.201700299.

[41] H.J. Butler, P.M. Brennan, J.M. Cameron, D. Finlayson, M.G. Hegarty, M.D. Jenkinson, D.S. Palmer, B.R. Smith, M.J. Baker, Development of high-throughput ATR-FTIR technology for rapid triage of brain cancer, Nat. Commun. 10 (2019) 1–9. https://doi.org/10.1038/s41467-019-12527-5.

[42] D.R. Parachalil, C. Bruno, F. Bonnier, H. Blasco, I. Chourpa, M.J. Baker, J. McIntyre, H.J. Byrne, Analysis of bodily fluids using vibrational spectroscopy: A direct comparison of Raman scattering and infrared absorption techniques for the case of glucose in blood serum, Analyst. 144 (2019) 3334–3346. https://doi.org/10.1039/c9an00125e.

[43] D.R. Parachalil, Screening of human serum/plasma using vibrational spectroscopy for early disease diagnostics and therapeutic drug monitoring, Technological University Dublin, 2019. https://doi.org/doi.org/10.21427/k6cy-n181.

[44] Y. Wang, B. Yan, L. Chen, SERS Tags: Novel optical nanoprobes for bioanalysis, Chem. Rev. 113 (2013) 1391–1428. https://doi.org/10.1021/cr300120g.

[45] Directive 2000/54/EC - biological agents at work | Safety and health at work EU-OSHA, (n.d.). https://osha.europa.eu/en/legislation/directives/exposure-to-biological-agents/77 (accessed

April 28, 2022).

[46]   Commission Directive (EU) 2020/739 of 3 June 2020 amending Annex III to Directive 2000/54/EC of the European Parliament and of the Council as regards the inclusion of SARS-CoV-2 in the list of biological agents known to infect humans and amending Commission Directive (EU) 2019/1833 - Publications Office of the EU, (n.d.). https://op.europa.eu/en/publication-detail/-/publication/26c2097f-a626-11ea-bb7a-01aa75ed71a1 (accessed April 28, 2022).

[47]   2020 Biological Agents Code of Practice Code of Practice for the Safety, Health and Welfare at Work (Biological Agents) Regulations 2013 and 2020, (n.d.).

[48]   S. Elveborg, V.M. Monteil, A. Mirazimi, Methods of Inactivation of Highly Pathogenic Viruses for Molecular, Serology or Vaccine Development Purposes, Pathogens. 11 (2022). https://doi.org/10.3390/PATHOGENS11020271.

[49]   P.L. Roberts, Virus inactivation by solvent/detergent treatment using Triton X-100 in a high purity factor VIII, Biologicals. 36 (2008) 330–335. https://doi.org/10.1016/J.BIOLOGICALS.2008.06.002.

[50]   J.A. Kiernan, Formaldehyde, Formalin, Paraformaldehyde And Glutaraldehyde: What They Are And What They Do, Micros. Today. 8 (2000) 8–13. https://doi.org/10.1017/S1551929500057060.

[51]   S.L. Park, Y.J.S. Huang, W.W. Hsu, S.M. Hettenbach, S. Higgs, D.L. Vanlandingham, Virus-specific thermostability and heat inactivation profiles of alphaviruses, J. Virol. Methods. 234 (2016) 152–155. https://doi.org/10.1016/J.JVIROMET.2016.04.004.

[52]   B. Ma, P.M. Gundy, C.P. Gerba, M.D. Sobsey, K.G. Linden, UV Inactivation of SARS-CoV-2 across the UVC Spectrum: KrCl* Excimer, Mercury-Vapor, and Light-Emitting-Diode (LED) Sources, Appl. Environ. Microbiol. 87 (2021). https://doi.org/10.1128/AEM.01532-21.

[53]   M.W. Beijerinck, Ueber ein contagium vivum fluidum als Ursache der Fleckenkrankheit der Tabaksblatter, Verh. Der K. Akad. van Wet. Te Amsterdam. (1898) 3–21.

[54]   H.-W. Ackermann, H.-W. Ackermann, The first phage electron micrographs, Bacteriophage. 1 (2011) 225–227. https://doi.org/10.4161/bact.1.4.17280.

[55]   W.M. Stanley, H.S. Loring, The Isolation of Crystalline Tobacco Mosaic Virus Protein from Diseased Tomato Plants, Science (80-.). 83 (1936) 85–85. https://doi.org/10.1126/science.83.2143.85.a.

[56]   W.M. Stanley, M.A. Lauffer, Disintegration of tobacco mosaic virus in urea solutions, Science (80-.). 89 (1939) 345–347. https://doi.org/10.1126/science.89.2311.345.

[57]   C.A. Knight, The Chemical Constitution of Viruses, Adv. Virus Res. 2 (1954) 153–182. https://doi.org/10.1016/S0065-3527(08)60532-1.

[58]   S. Subramaniam, A. Bartesaghi, J. Liu, A.E. Bennett, R. Sougrat, Electron tomography of viruses, Curr. Opin. Struct. Biol. 17 (2007) 596–602. https://doi.org/10.1016/j.sbi.2007.09.009.

[59]   W. Jiang, L. Tang, Atomic cryo-EM structures of viruses, Curr. Opin. Struct. Biol. 46 (2017) 122–129. https://doi.org/10.1016/J.SBI.2017.07.002.

[60]   H.R. Gelderblom, Structure and Classification of Viruses, Med. Microbiol. (1996). https://pubmed.ncbi.nlm.nih.gov/21413309/ (accessed December 29, 2021).

[61] K.R. Richert-Pöggeler, K. Franzke, K. Hipp, R.G. Kleespies, Electron microscopy methods for virus diagnosis and high resolution analysis of viruses, Front. Microbiol. 10 (2019) 3255. https://doi.org/10.3389/fmicb.2018.03255.

[62] A. Milewska, J. Ner-Kluza, A. Dabrowska, A. Bodzon-Kulakowska, K. Pyrc, P. Suder, MASS SPECTROMETRY IN VIROLOGICAL SCIENCES, Mass Spectrom. Rev. 39 (2020) 499–522. https://doi.org/10.1002/mas.21617.

[63] W. Surya, Y. Li, J. Torres, Structural model of the SARS coronavirus E channel in LMPG micelles, Biochim. Biophys. Acta - Biomembr. 1860 (2018) 1309–1317. https://doi.org/10.1016/j.bbamem.2018.02.017.

[64] R.K. Koppisetti, Y.G. Fulcher, A. Jurkevich, S.H. Prior, J. Xu, M. Lenoir, M. Overduin, S.R. Van Doren, Ambidextrous binding of cell and membrane bilayers by soluble matrix metalloproteinase-12, Nat. Commun. 5 (2014) 1–14. https://doi.org/10.1038/ncomms6552.

[65] H. Yao, Y. Song, Y. Chen, N. Wu, J. Xu, C. Sun, J. Zhang, T. Weng, Z. Zhang, Z. Wu, L. Cheng, D. Shi, X. Lu, J. Lei, M. Crispin, Y. Shi, L. Li, S. Li, Molecular Architecture of the SARS-CoV-2 Virus, Cell. 183 (2020) 730-738.e13. https://doi.org/10.1016/j.cell.2020.09.018.

[66] M. Oostra, C.A.M. de Haan, R.J. de Groot, P.J.M. Rottier, Glycosylation of the Severe Acute Respiratory Syndrome Coronavirus Triple-Spanning Membrane Proteins 3a and M, J. Virol. 80 (2006) 2326–2336. https://doi.org/10.1128/jvi.80.5.2326-2336.2006.

[67] B.W. Neuman, M.J. Buchmeier, Supramolecular Architecture of the Coronavirus Particle, in: Adv. Virus Res., Adv Virus Res, 2016: pp. 1–27. https://doi.org/10.1016/bs.aivir.2016.08.005.

[68] B.W. Neuman, G. Kiss, A.H. Kunding, D. Bhella, M.F. Baksh, S. Connelly, B. Droese, J.P. Klaus, S. Makino, S.G. Sawicki, S.G. Siddell, D.G. Stamou, I.A. Wilson, P. Kuhn, M.J. Buchmeier, A structural analysis of M protein in coronavirus assembly and morphology, J. Struct. Biol. 174 (2011) 11–22. https://doi.org/10.1016/j.jsb.2010.11.021.

[69] A. Yu, A.J. Pak, P. He, V. Monje-Galvan, L. Casalino, Z. Gaieb, A.C. Dommer, R.E. Amaro, G.A. Voth, A multiscale coarse-grained model of the SARS-CoV-2 virion, Biophys. J. 120 (2021) 1097–1104. https://doi.org/10.1016/j.bpj.2020.10.048.

[70] Y.K. Choi, Y. Cao, M. Frank, H. Woo, S.J. Park, M.S. Yeom, T.I. Croll, C. Seok, W. Im, Structure, Dynamics, Receptor Binding, and Antibody Binding of the Fully Glycosylated Full-Length SARS-CoV-2 Spike Protein in a Viral Membrane, J. Chem. Theory Comput. 17 (2021) 2479–2487. https://doi.org/10.1021/acs.jctc.0c01144.

[71] S.S. Hwang, J. Lim, Z. Yu, P. Kong, E. Sefik, H. Xu, C.C.D. Harman, L.K. Kim, G.R. Lee, H.B. Li, R.A. Flavell, MRNA destabilization by BTG1 and BTG2 maintains T cell quiescence, Science (80-.). 367 (2020) 1255–1260. https://doi.org/10.1126/science.abb2507.

[72] H.S. Hillen, G. Kokic, L. Farnung, C. Dienemann, D. Tegunov, P. Cramer, Structure of replicating SARS-CoV-2 polymerase, Nature. 584 (2020) 154–156. https://doi.org/10.1038/s41586-020-2368-8.

[73] L.J. Harris, S.B. Larson, K.W. Hasel, A. McPherson, Refined structure of an intact IgG2a monoclonal antibody, Biochemistry. 36 (1997) 1581–1597. https://doi.org/10.1021/bi962514+.

[74] S. Noreng, A. Bharadwaj, R. Posert, C. Yoshioka, I. Baconguis, Structure of the human epithelial sodium channel by cryo-electron microscopy, Elife. 7 (2018). https://doi.org/10.7554/eLife.39340.

[75] A. Almond, P.L. DeAngelis, C.D. Blundell, Hyaluronan: The Local Solution Conformation Determined by NMR and Computer Modeling is Close to a Contracted Left-handed 4-Fold Helix, J. Mol. Biol. 358 (2006) 1256–1269. https://doi.org/10.1016/j.jmb.2006.02.077.

[76] D.L. Hurdiss, I. Drulyte, Y. Lang, T.M. Shamorkina, M.F. Pronker, F.J.M. van Kuppeveld, J. Snijder, R.J. de Groot, Cryo-EM structure of coronavirus-HKU1 haemagglutinin esterase reveals architectural changes arising from prolonged circulation in humans, Nat. Commun. 11 (2020) 1–10. https://doi.org/10.1038/s41467-020-18440-6.

[77] R. Yan, Y. Zhang, Y. Li, L. Xia, Y. Guo, Q. Zhou, Structural basis for the recognition of SARS-CoV-2 by full-length human ACE2, Science (80-.). 367 (2020) 1444–1448. https://doi.org/10.1126/science.abb2762.

[78] G. Javitt, L. Khmelnitsky, L. Albert, L.S. Bigman, N. Elad, D. Morgenstern, T. Ilani, Y. Levy, R. Diskin, D. Fass, Assembly Mechanism of Mucin and von Willebrand Factor Polymers, Cell. 183 (2020) 717-729.e16. https://doi.org/10.1016/j.cell.2020.09.021.

[79] M.Y. Wang, R. Zhao, L.J. Gao, X.F. Gao, D.P. Wang, J.M. Cao, SARS-CoV-2: Structure, Biology, and Structure-Based Therapeutics Development, Front. Cell. Infect. Microbiol. 10 (2020). https://doi.org/10.3389/fcimb.2020.587269.

[80] C.A. Vargas, A.A. Wilhelm, J. Williams, P. Lucas, K.A. Reynolds, M.R. Riley, Integrated capture and spectroscopic detection of viruses, Appl. Environ. Microbiol. 75 (2009) 6431–6440. https://doi.org/10.1128/AEM.02036-08.

[81] S. Gamage, M. Howard, H. Makita, B. Cross, G. Hastings, M. Luo, Y. Abate, Probing structural changes in single enveloped virus particles using nano-infrared spectroscopic imaging, PLoS One. 13 (2018) e0199112. https://doi.org/10.1371/journal.pone.0199112.

[82] K.A. Hartman, P.E. McDonald-Ordzie, J.M. Kaper, B. Prescott, G.J. Thomas, Studies of Virus Structure by Laser-Raman Spectroscopy. Turnip Yellow Mosaic Virus and Capsids, Biochemistry. 17 (1978) 2118–2123. https://doi.org/10.1021/bi00604a015.

[83] B. Prescott, G.J. Thomas, K. Sitaraman, P. Argos, Protein-RNA Interactions in Belladonna Mottle Virus Investigated by Laser Raman Spectroscopy, Biochemistry. 24 (1985) 1226–1231. https://doi.org/10.1021/bi00326a026.

[84] T. Li, Z. Chen, J.E. Johnson, G.J. Thomas, T. Li, Z. Chen, J.E. Johnson, G.J. Thomas, Structural Studies of Bean Pod Mottle Virus, Capsid, and RNA in Crystal and Solution States by Laser Raman Spectroscopy, Biochemistry. 29 (1990) 5018–5026. https://doi.org/10.1021/bi00473a004.

[85] T. Li, J.E. Johnson, G.J. Thomas, Raman dynamic probe of hydrogen exchange in bean pod mottle virus: base-specific retardation of exchange in packaged ssRNA, Biophys. J. 65 (1993) 1963–1972. https://doi.org/10.1016/S0006-3495(93)81272-4.

[86] S.A. Overman, K.L. Aubrey, N.S. Vispo, G. Cesareni, G.J. Thomas, Novel Tyrosine Markers in Raman Spectra of Wild-Type and Mutant (Y21M and Y24M) Ff Virions Indicate Unusual Environments for Coat Protein Phenoxyls, Biochemistry. 33 (1994) 1037–1042. https://doi.org/10.1021/bi00171a001.

[87] S.A. Overman, G.J. Thomas, Raman Spectroscopy of the Filamentous Virus Ff (fd, f1, M13): Structural Interpretation for Coat Protein Aromatics, Biochemistry. 34 (1995) 5440–5451. https://doi.org/10.1021/bi00016a015.

[88] S.R. Fish, K.A. Hartman, M.T. Fuller, J. King, G.J. Thomas, Investigation of secondary structures and macromolecular interactions in bacteriophage p22 by laser raman spectroscopy, Biophys.

J. 32 (1980) 234–237. https://doi.org/10.1016/S0006-3495(80)84945-9.

[89] R. Tuma, J.H.K. Bamford, D.H. Bamford, G.J. Thomas, Structure, interactions and dynamics of PRD1 virus II. Organization of the viral membrane and DNA, J. Mol. Biol. 257 (1996) 102–115. https://doi.org/10.1006/jmbi.1996.0150.

[90] Y. Xu, C. Lu, Raman spectroscopic study on structure of human immunodeficiency virus (HIV) and hypericin-induced photosensitive damage of HIV, Sci. China Ser. C Life Sci. 48 (2005) 117–132. https://doi.org/10.1007/bf02879664.

[91] P. Ruokola, E. Dadu, A. Kazmertsuk, H. Hakkanen, V. Marjomaki, J.A. Ihalainen, Raman Spectroscopic Signatures of Echovirus 1 Uncoating, J. Virol. 88 (2014) 8504–8513. https://doi.org/10.1128/jvi.03398-13.

[92] P. Di Bao, T.Q. Huang, X.M. Liu, T.Q. Wu, Surface-enhanced Raman spectroscopy of insect nuclear polyhedrosis virus, J. Raman Spectrosc. 32 (2001) 227–230. https://doi.org/10.1002/jrs.665.

[93] S. Shanmukh, L. Jones, J. Driskell, Y. Zhao, R. Dluhy, R.A. Tripp, Rapid and sensitive detection of respiratory virus molecular signatures using a silver nanorod array SERS substrate, Nano Lett. 6 (2006) 2630–2636. https://doi.org/10.1021/nl061666f.

[94] R.A. Dluhy, S. Shanmukh, L. Jones, Y.P. Zhao, J.D. Driskell, R.A. Tripp, Identification and classification of respiratory syncytial virus (RSV) strains by surface-enhanced Raman spectroscopy and multivariate statistical techniques, Anal. Bioanal. Chem. 390 (2008) 1551–1555. https://doi.org/10.1007/s00216-008-1851-0.

[95] J.D. Driskell, Y. Zhu, C.D. Kirkwood, Y. Zhao, R.A. Dluhy, R.A. Tripp, Rapid and sensitive detection of rotavirus molecular signatures using surface enhanced raman spectroscopy, PLoS One. 5 (2010) e10222. https://doi.org/10.1371/journal.pone.0010222.

[96] M. Rippa, R. Castagna, S. Brandi, G. Fusco, M. Monini, D. Chen, J. Zhou, J. Zyss, L. Petti, Octupolar Plasmonic Nanosensor Based on Ordered Arrays of Triangular Au Nanopillars for Selective Rotavirus Detection, ACS Appl. Nano Mater. 3 (2020) 4837–4844. https://doi.org/10.1021/acsanm.0c00872.

[97] T.A. Alexander, Development of methodology based on commercialized SERS-active substrates for rapid discrimination of Poxviridae virions, Anal. Chem. 80 (2008) 2817–2825. https://doi.org/10.1021/ac702464w.

[98] C. Fan, Z. Hu, L.K. Riley, G.A. Purdy, A. Mustapha, M. Lin, Detecting food- and waterborne viruses by surface-enhanced raman spectroscopy, J. Food Sci. 75 (2010). https://doi.org/10.1111/j.1750-3841.2010.01619.x.

[99] K. Olschewski, E. Kämmer, S. Stöckel, T. Bocklitz, T. Deckert-Gaudig, R. Zell, D. Cialla-May, K. Weber, V. Deckert, J. Popp, A manual and an automatic TERS based virus discrimination, Nanoscale. 7 (2015) 4545–4552. https://doi.org/10.1039/c4nr07033j.

[100] J.D. Driskell, K.M. Kwarta, R.J. Lipert, M.D. Porter, J.D. Neill, J.F. Ridpath, Low-level detection of viral pathogens by a surface-enhanced Raman scattering based immunoassay, Anal. Chem. 77 (2005) 6147–6154. https://doi.org/10.1021/ac0504159.

[101] M. Sánchez-Purrà, M. Carré-Camps, H. De Puig, I. Bosch, L. Gehrke, K. Hamad-Schifferli, Surface-Enhanced Raman Spectroscopy-Based Sandwich Immunoassays for Multiplexed Detection of Zika and Dengue Viral Biomarkers, ACS Infect. Dis. 3 (2017) 767–776. https://doi.org/10.1021/acsinfecdis.7b00110.

[102] M. Sánchez-Purrà, B. Roig-Solvas, A. Versiani, C. Rodriguez-Quijada, H. De Puig, I. Bosch, L. Gehrke, K. Hamad-Schifferli, Design of SERS nanotags for multiplexed lateral flow immunoassays, Mol. Syst. Des. Eng. 2 (2017) 401–409. https://doi.org/10.1039/c7me00052a.

[103] A.M. Paul, Z. Fan, S.S. Sinha, Y. Shi, L. Le, F. Bai, P.C. Ray, Bioconjugated Gold Nanoparticle Based SERS Probe for Ultrasensitive Identification of Mosquito-Borne Viruses Using Raman Fingerprinting, J. Phys. Chem. C. 119 (2015) 23669–23675. https://doi.org/10.1021/acs.jpcc.5b07387.

[104] K. Sivashanmugan, H. Lee, J. Der Liao, C.C. Wang, C.H. Lin, Y.S. Yang, J. Sitjar, Mutated human p-selectin glycoprotein ligand-1 and viral protein-1 of enterovirus 71 interactions on Au nanoplasmonic substrate for specific recognition by surface-enhanced raman spectroscopy, Coatings. 10 (2020) 403. https://doi.org/10.3390/coatings10040403.

[105] O. Ambartsumyan, D. Gribanyov, V. Kukushkin, A. Kopylov, E. Zavyalova, SERS-based biosensors for virus determination with oligonucleotides as recognition elements, Int. J. Mol. Sci. 21 (2020). https://doi.org/10.3390/ijms21093373.

[106] Y.T. Yeh, K. Gulino, Y.H. Zhang, A. Sabestien, T.W. Chou, B. Zhou, Z. Lin, I. Albert, H. Lu, V. Swaminathan, E. Ghedin, M. Terrones, A rapid and label-free platform for virus capture and identification from clinical samples, Proc. Natl. Acad. Sci. U. S. A. 117 (2020) 895–901. https://doi.org/10.1073/pnas.1910113117.

[107] M.S. Maginnis, Virus–Receptor Interactions: The Key to Cellular Invasion, J. Mol. Biol. 430 (2018) 2590–2611. https://doi.org/10.1016/j.jmb.2018.06.024.

[108] S. V. Barrass, S.J. Butcher, Advances in high-throughput methods for the identification of virus receptors, Med. Microbiol. Immunol. 209 (2020) 309–323. https://doi.org/10.1007/s00430-019-00653-2.

[109] R.J. Colonno, P.L. Callahan, W.J. Long, Isolation of a monoclonal antibody that blocks attachment of the major group of human rhinoviruses, J. Virol. 57 (1986) 7–12. https://doi.org/10.1128/jvi.57.1.7-12.1986.

[110] G.N. Gaulton, M.S. Co, H.D. Royer, M.I. Greene, Anti-idiotypic antibodies as probes of cell surface receptors, Mol. Cell. Biochem. 65 (1984) 5–21. https://doi.org/10.1007/BF00226015.

[111] D.L. Krah, R.L. Crowell, A solid-phase assay of solubilized HeLa cell membrane receptors for binding group B coxsackieviruses and polioviruses, Virology. 118 (1982) 148–156. https://doi.org/10.1016/0042-6822(82)90328-2.

[112] E. V. Protopopova, A. V. Sorokin, S.N. Konovalova, A. V. Kachko, S. V. Netesov, V.B. Loktev, Human laminin binding protein as a cell receptor for the tick-borne encephalitis virus, Zentralblatt Fur Bakteriol. 289 (1999) 632–638. https://doi.org/10.1016/S0934-8840(99)80021-8.

[113] A. Michalski, E. Damoc, O. Lange, E. Denisov, D. Nolting, M. Müller, R. Viner, J. Schwartz, P. Remes, M. Belford, J.J. Dunyach, J. Cox, S. Horning, M. Mann, A. Makarov, Ultra high resolution linear ion trap orbitrap mass spectrometer (orbitrap elite) facilitates top down LC MS/MS and versatile peptide fragmentation modes, Mol. Cell. Proteomics. 11 (2012). https://doi.org/10.1074/mcp.O111.013698.

[114] K. Bösl, A. Ianevski, T.T. Than, P.I. Andersen, S. Kuivanen, M. Teppor, E. Zusinaite, U. Dumpis, A. Vitkauskiene, R.J. Cox, H. Kallio-Kokko, A. Bergqvist, T. Tenson, A. Merits, V. Oksenych, M. Bjørås, M.W. Anthonsen, D. Shum, M. Kaarbø, O. Vapalahti, M.P. Windisch, G. Superti-Furga, B. Snijder, D. Kainov, R.K. Kandasamy, Common Nodes of Virus–Host Interaction Revealed

Through an Integrated Network Analysis, Front. Immunol. 10 (2019) 2186. https://doi.org/10.3389/fimmu.2019.02186.

[115] Y. Hatta, K. Hershberger, K. Shinya, S.C. Proll, R.R. Dubielzig, M. Hatta, M.G. Katze, Y. Kawaoka, M. Suresh, Viral replication rate regulates clinical outcome and CD8 T Cell responses during highly pathogenic H5N1 influenza virus infection in mice, PLoS Pathog. 6 (2010) 1001139. https://doi.org/10.1371/journal.ppat.1001139.

[116] I.M. Mackay, K.E. Arden, A. Nitsche, Real-time PCR in virology, Nucleic Acids Res. 30 (2002) 1292–1305. https://doi.org/10.1093/nar/30.6.1292.

[117] I. Castillo, E. Rodríguez-Iñigo, J. Bartolomé, S. De Lucas, N. Ortíz-Movilla, J.M. López-Alcorocho, M. Pardo, V. Carreño, Hepatitis C virus replicates in peripheral blood mononuclear cells of patients with occult hepatitis C virus infection, Gut. 54 (2005) 682–685. https://doi.org/10.1136/gut.2004.057281.

[118] X. Xie, M. Pang, S. Liang, Y. Lin, Y. Zhao, D. Qiu, J. Liu, Y. Dong, Y. Liu, Cellular microRNAs influence replication of H3N2 canine influenza virus in infected cells, Vet. Microbiol. 257 (2021). https://doi.org/10.1016/j.vetmic.2021.109083.

[119] L. Garibyan, N. Avashia, Polymerase chain reaction, J. Invest. Dermatol. 133 (2013) 1–4. https://doi.org/10.1038/jid.2013.1.

[120] S. Culley, G.J. Towers, D.L. Selwood, R. Henriques, J. Grove, Infection counter: Automated quantification of in vitro virus replication by fluorescence microscopy, Viruses. 8 (2016). https://doi.org/10.3390/v8070201.

[121] A.M. Copeland, W.W. Newcomb, J.C. Brown, Herpes Simplex Virus Replication: Roles of Viral Proteins and Nucleoporins in Capsid-Nucleus Attachment, J. Virol. 83 (2009) 1660–1668. https://doi.org/10.1128/jvi.01139-08.

[122] R. Bolten, D. Egger, R. Gosert, G. Schaub, L. Landmann, K. Bienz, Intracellular Localization of Poliovirus Plus- and Minus-Strand RNA Visualized by Strand-Specific Fluorescent In Situ Hybridization, J. Virol. 72 (1998) 8578–8585. https://doi.org/10.1128/jvi.72.11.8578-8585.1998.

[123] X. Lu, Q. Liu, J.A. Benavides-Montano, A. V. Nicola, D.E. Aston, B.A. Rasco, H.C. Aguilar, Detection of Receptor-Induced Glycoprotein Conformational Changes on Enveloped Virions by Using Confocal Micro-Raman Spectroscopy, J. Virol. 87 (2013) 3130–3142. https://doi.org/10.1128/jvi.03220-12.

[124] M. Huleihel, V. Erukhimovitch, M. Talyshinsky, M. Karpasas, Spectroscopic characterization of normal primary and malignant cells transformed by retroviruses, Appl. Spectrosc. 56 (2002) 640–645. https://doi.org/10.1366/0003702021955204.

[125] A. Salman, V. Erukhimovitch, M. Talyshinsky, M. Huleihil, M. Huleihel, FTIR spectroscopic method for detection of cells infected with herpes viruses, Biopolym. - Biospectroscopy Sect. 67 (2002) 406–412. https://doi.org/10.1002/bip.10171.

[126] P. Bassan, H.J. Byrne, J. Lee, F. Bonnier, C. Clarke, P. Dumas, E. Gazi, M.D. Brown, N.W. Clarke, P. Gardner, Reflection contributions to the dispersion artefact in FTIR spectra of single biological cells, Analyst. 134 (2009) 1171–1175. https://doi.org/10.1039/b821349f.

[127] P. Bassan, H.J. Byrne, F. Bonnier, J. Lee, P. Dumas, P. Gardner, Resonant Mie scattering in infrared spectroscopy of biological materials - Understanding the "dispersion artefact," Analyst. 134 (2009) 1586–1593. https://doi.org/10.1039/b904808a.

[128] K.M. Ostrowska, A. Garcia, A.D. Meade, A. Malkin, I. Okewumi, J.J. O'Leary, C. Martin, H.J. Byrne, F.M. Lyng, Correlation of p16INK4A expression and HPV copy number with cellular FTIR spectroscopic signatures of cervical cancer cells, Analyst. 136 (2011) 1365–1373. https://doi.org/10.1039/c0an00910e.

[129] V. Erukhimovitch, I. Mukmanov, M. Talyshinsky, Y. Souprun, M. Huleihel, The use of FTIR microscopy for evaluation of herpes viruses infection development kinetics, Spectrochim. Acta - Part A Mol. Biomol. Spectrosc. 60 (2004) 2355–2361. https://doi.org/10.1016/j.saa.2003.12.009.

[130] A.C.S. Talari, Z. Movasaghi, S. Rehman, I.U. Rehman, Raman Spectroscopy of Biological Tissues, Http://Dx.Doi.Org/10.1080/05704928.2014.923902. 50 (2014) 46–111. https://doi.org/10.1080/05704928.2014.923902.

[131] V. Erukhimovitch, E. Bogomolny, M. Huleihil, M. Huleihel, Infrared spectral changes identified during different stages of herpes viruses infection in vitro, Analyst. 136 (2011) 2818–2824. https://doi.org/10.1039/c1an15319f.

[132] G. Hastings, P. Krug, R. Wang, J. Guo, H.P. Lamichhane, T. Tang, Y.S. Hsu, J. Ward, D. Katz, J. Hilliard, Viral infection of cells in culture detected using infrared microscopy, Analyst. 134 (2009) 1462–1471. https://doi.org/10.1039/b902154j.

[133] J.G. Kelly, K.T. Cheung, C. Martin, J.J. O'Leary, W. Prendiville, P.L. Martin-Hirsch, F.L. Martin, A spectral phenotype of oncogenic human papillomavirus-infected exfoliative cervical cytology distinguishes women based on age, Clin. Chim. Acta. 411 (2010) 1027–1033. https://doi.org/10.1016/j.cca.2010.03.029.

[134] K.M. Ostrowska, A. Malkin, A. Meade, J. O'Leary, C. Martin, C. Spillane, H.J. Byrne, F.M. Lyng, Investigation of the influence of high-risk human papillomavirus on the biochemical composition of cervical cancer cells using vibrational spectroscopy, Analyst. 135 (2010) 3087–3093. https://doi.org/10.1039/c0an00571a.

[135] F.T. Lee-Montiel, K.A. Reynolds, M.R. Riley, Detection and quantification of poliovirus infection using FTIR spectroscopy and cell culture, J. Biol. Eng. 5 (2011) 16. https://doi.org/10.1186/1754-1611-5-16.

[136] K.M.G. Lima, K. Gajjar, G. Valasoulis, M. Nasioutziki, M. Kyrgiou, P. Karakitsos, E. Paraskevaidis, P.L. Martin Hirsch, F.L. Martin, Classification of cervical cytology for human papilloma virus (HPV) infection using biospectroscopy and variable selection techniques, Anal. Methods. 6 (2014) 9643–9652. https://doi.org/10.1039/c4ay01736f.

[137] K.E. Hamden, B.A. Bryan, P.W. Ford, C. Xie, Y.Q. Li, S.M. Akula, Spectroscopic analysis of Kaposi's sarcoma-associated herpesvirus infected cells by Raman tweezers, J. Virol. Methods. 129 (2005) 145–151. https://doi.org/10.1016/j.jviromet.2005.05.018.

[138] O.F. Dyson, P.W. Ford, D. Chen, Y.Q. Li, S.M. Akula, Raman tweezers provide the fingerprint of cells supporting the late stages of KSHV reactivation, J. Cell. Mol. Med. 13 (2009) 1920–1932. https://doi.org/10.1111/j.1582-4934.2008.00481.x.

[139] A. Salman, E. Shufan, L. Zeiri, M. Huleihel, Characterization and detection of Vero cells infected with Herpes Simplex Virus type 1 using Raman spectroscopy and advanced statistical methods, Methods. 68 (2014) 364–370. https://doi.org/10.1016/j.ymeth.2014.02.022.

[140] M. Huleihel, E. Shufan, L. Zeiri, A. Salman, Detection of vero cells infected with herpes simplex types 1 and 2 and varicella zoster viruses using raman spectroscopy and advanced statistical methods, PLoS One. 11 (2016) e0153599. https://doi.org/10.1371/journal.pone.0153599.

[141] N.A. Odintsova, M.G. Eliseikina, T. V. Ryazanova, Experimental infection of king crab hemocytes with a herpes-like virus in culture, Russ. J. Mar. Biol. 41 (2015) 401–404. https://doi.org/10.1134/S1063074015050107.

[142] J.Y. Lim, J.S. Nam, H. Shin, J. Park, H.I. Song, M. Kang, K. Il Lim, Y. Choi, Identification of Newly Emerging Influenza Viruses by Detecting the Virally Infected Cells Based on Surface Enhanced Raman Spectroscopy and Principal Component Analysis, Anal. Chem. 91 (2019) 5677–5684. https://doi.org/10.1021/acs.analchem.8b05533.

[143] K. Moor, K. Ohtani, D. Myrzakozha, O. Zhanserkenova, B.B. Andriana, H. Sato, Noninvasive and label-free determination of virus infected cells by Raman spectroscopy, J. Biomed. Opt. 19 (2014) 067003. https://doi.org/10.1117/1.jbo.19.6.067003.

[144] K. Moor, Y. Terada, A. Taketani, H. Matsuyoshi, K. Ohtani, Early detection of virus infection in live human cells using Raman spectroscopy, J. Biomed. Opt. 23 (2018) 1. https://doi.org/10.1117/1.jbo.23.9.097001.

[145] G. Pezzotti, W. Zhu, T. Adachi, S. Horiguchi, E. Marin, F. Boschetto, E. Ogitani, O. Mazda, Metabolic machinery encrypted in the Raman spectrum of influenza A virus-inoculated mammalian cells, J. Cell. Physiol. 235 (2020) 5146–5170. https://doi.org/10.1002/jcp.29392.

[146] D. Tiwari, S. Jakhmola, D.K. Pathak, R. Kumar, H.C. Jha, Temporal in Vitro Raman Spectroscopy for Monitoring Replication Kinetics of Epstein-Barr Virus Infection in Glial Cells, ACS Omega. 5 (2020) 29547–29560. https://doi.org/10.1021/acsomega.0c04525.

[147] J.B. Luchansky, Publication : USDA ARS Publication : USDA ARS, in: Symp. Proc., 2017: pp. 7–8. https://www.ars.usda.gov/research/publications/publication/?seqNo115=269051.

[148] X. Liu, J.E. Grice, J. Lademann, N. Otberg, S. Trauer, A. Patzelt, M.S. Roberts, Hair follicles contribute significantly to penetration through human skin only at times soon after application as a solvent deposited solid in man, Br. J. Clin. Pharmacol. 72 (2011) 768–774. https://doi.org/10.1111/j.1365-2125.2011.04022.x.

[149] P.G. Choe, K.H. Kim, C.K. Kang, H.J. Suh, E.K. Kang, S.Y. Lee, N.J. Kim, J. Yi, W.B. Park, M.D. Oh, Antibody responses 8 months after asymptomatic or mild SARS-CoV-2 infection, Emerg. Infect. Dis. 27 (2021) 928–931. https://doi.org/10.3201/eid2703.204543.

[150] Lateral flow devices detect most infectious COVID-19 cases and could allow a safer relaxation of the current lockdown | University of Oxford, (n.d.). https://www.ox.ac.uk/news/2021-01-21-lateral-flow-devices-detect-most-infectious-covid-19-cases-and-could-allow-safer.

[151] M. Pavelka, K. Van-Zandvoort, S. Abbott, K. Sherratt, M. Majdan, P. Jarčuška, M. Krajčí, S. Flasche, S. Funk, The impact of population-wide rapid antigen testing on SARS-CoV-2 prevalence in Slovakia, Science (80-.). 372 (2021) 635–641. https://doi.org/10.1126/science.abf9648.

[152] V.K. Shah, P. Firmal, A. Alam, D. Ganguly, S. Chattopadhyay, Overview of Immune Response During SARS-CoV-2 Infection: Lessons From the Past, Front. Immunol. 11 (2020). https://doi.org/10.3389/fimmu.2020.01949.

[153] G.E. Hartley, E.S.J. Edwards, P.M. Aui, N. Varese, S. Stojanovic, J. McMahon, A.Y. Peleg, I. Boo, H.E. Drummer, P.M. Hogarth, R.E. O'Hehir, M.C. van Zelm, Rapid generation of durable B cell memory to SARS-CoV-2 spike and nucleocapsid proteins in COVID-19 and convalescence, Sci. Immunol. 5 (2020). https://doi.org/10.1126/sciimmunol.abf8891.

[154] A. Hamady, J.J. Lee, Z.A. Loboda, Waning antibody responses in COVID-19: what can we learn from the analysis of other coronaviruses?, Infection. 1 (2021) 1.

https://doi.org/10.1007/s15010-021-01664-z.

[155] Y. Galipeau, M. Greig, G. Liu, M. Driedger, M.A. Langlois, Humoral Responses and Serological Assays in SARS-CoV-2 Infections, Front. Immunol. 11 (2020) 3382. https://doi.org/10.3389/fimmu.2020.610688.

[156] T. Jaenisch, D.T.H. Tam, N.T.T. Kieu, T. Ngoc, N.T. Nam, N. Van Kinh, S. Yacoub, N. Chanpheaktra, V. Kumar, L.L.C. See, J. Sathar, E.P. Sandoval, G.M.M. Alfaro, I.S. Laksono, Y. Mahendradhata, M. Sarker, F. Ahmed, A. Caprara, B.S. Benevides, E.T.A. Marques, T. Magalhaes, P. Brasil, M. Netto, A. Tami, S.E. Bethencourt, M. Guzman, C. Simmons, N.T.H. Quyen, L. Merson, N.T.P. Dung, D. Beck, M. Wirths, M. Wolbers, P.K. Lam, K. Rosenberger, B. Wills, Clinical evaluation of dengue and identification of risk factors for severe disease: Protocol for a multicentre study in 8 countries, BMC Infect. Dis. 16 (2016). https://doi.org/10.1186/s12879-016-1440-3.

[157] S. Roy, D. Perez-Guaita, S. Bowden, P. Heraud, B.R. Wood, Spectroscopy goes viral: Diagnosis of hepatitis B and C virus infection from human sera using ATR-FTIR spectroscopy, Clin. Spectrosc. 1 (2019) 100001. https://doi.org/10.1016/j.clispe.2020.100001.

[158] L.G. Silva, A.F.S. Péres, D.L.D. Freitas, C.L.M. Morais, F.L. Martin, J.C.O. Crispim, K.M.G. Lima, ATR-FTIR spectroscopy in blood plasma combined with multivariate analysis to detect HIV infection in pregnant women, Sci. Rep. 10 (2020) 1–7. https://doi.org/10.1038/s41598-020-77378-3.

[159] I.M. Alves Melo, M.R. Pereira Viana, B. Pupin, T.T. Bhattacharjee, R. de Azevedo Canevari, PCR-RFLP and FTIR-based detection of high-risk human papilloma virus for cervical cancer screening and prevention, Biochem. Biophys. Reports. 26 (2021) 100993. https://doi.org/10.1016/j.bbrep.2021.100993.

[160] T. Mahmood, H. Nawaz, A. Ditta, M.I. Majeed, M.A. Hanif, N. Rashid, H.N. Bhatti, H.F. Nargis, M. Saleem, F. Bonnier, H.J. Byrne, Raman spectral analysis for rapid screening of dengue infection, Spectrochim. Acta - Part A Mol. Biomol. Spectrosc. 200 (2018) 136–142. https://doi.org/10.1016/j.saa.2018.04.018.

[161] M. Saleem, M. Bilal, S. Anwar, A. Rehman, M. Ahmed, Optical diagnosis of dengue virus infection in human blood serum using Raman spectroscopy, Laser Phys. Lett. 10 (2013) 1–5. https://doi.org/10.1088/1612-2011/10/3/035602.

[162] S. Khan, R. Ullah, A. Khan, N. Wahab, M. Bilal, M. Ahmed, Analysis of dengue infection based on Raman spectroscopy and support vector machine (SVM), Biomed. Opt. Express. 7 (2016) 2249. https://doi.org/10.1364/boe.7.002249.

[163] M. Bilal, M. Saleem, M. Bilal, T. Ijaz, S. Khan, R. Ullah, A. Raza, M. Khurram, W. Akram, M. Ahmed, Raman spectroscopy-based screening of IgM positive and negative sera for dengue virus infection, Laser Phys. 26 (2016) 115602. https://doi.org/10.1088/1054-660X/26/11/115602.

[164] H. Nawaz, N. Rashid, M. Saleem, M. Asif Hanif, M. Irfan Majeed, I. Amin, M. Iqbal, M. Rahman, O. Ibrahim, S.M. Baig, M. Ahmed, F. Bonnierg, H.J. Byrnee, Prediction of viral loads for diagnosis of hepatitis C infection in human plasma samples using raman spectroscopy coupled with partial least squares regression analysis, J. Raman Spectrosc. 48 (2017) 697–704. https://doi.org/10.1002/jrs.5108.

[165] W.A. El-Said, J. woo Choi, High selective spectroelectrochemical biosensor for HCV-RNA detection based on a specific peptide nucleic acid, Spectrochim. Acta - Part A Mol. Biomol. Spectrosc. 217 (2019) 288–293. https://doi.org/10.1016/j.saa.2019.03.115.

[166] F. Batool, H. Nawaz, M.I. Majeed, N. Rashid, S. Bashir, S. Akbar, M. Abubakar, S. Ahmad, M.N. Ashraf, S. Ali, M. Kashif, I. Amin, SERS-based viral load quantification of hepatitis B virus from PCR products, Spectrochim. Acta - Part A Mol. Biomol. Spectrosc. 255 (2021). https://doi.org/10.1016/j.saa.2021.119722.

[167] S. Nasir, M.I. Majeed, H. Nawaz, N. Rashid, S. Ali, S. Farooq, M. Kashif, S. Rafiq, S. Bano, M.N. Ashraf, M. Abubakar, S. Ahmad, A. Rehman, I. Amin, Surface enhanced Raman spectroscopy of RNA samples extracted from blood of hepatitis C patients for quantification of viral loads, Photodiagnosis Photodyn. Ther. 33 (2021). https://doi.org/10.1016/j.pdpdt.2020.102152.

[168] L.F. das C. e. S. de Carvalho, M.S. Nogueira, Optical techniques for fast screening – Towards prevention of the coronavirus COVID-19 outbreak, Photodiagnosis Photodyn. Ther. 30 (2020) 101765. https://doi.org/10.1016/j.pdpdt.2020.101765.

[169] D. Graham, Can raman spectroscopy be a useful tool in the fight against COVID-19?, Spectrosc. (Santa Monica). 35 (2020) 44–46.

[170] R.S. Khan, I.U. Rehman, Spectroscopy as a tool for detection and monitoring of Coronavirus (COVID-19), Expert Rev. Mol. Diagn. 20 (2020) 647–649. https://doi.org/10.1080/14737159.2020.1766968.

[171] J. Lukose, S. Chidangil, S.D. George, Optical technologies for the detection of viruses like COVID-19: Progress and prospects, Biosens. Bioelectron. 178 (2021) 113004. https://doi.org/10.1016/j.bios.2021.113004.

[172] P. Heraud, P. Chatchawal, M. Wongwattanakul, P. Tippayawat, C. Doerig, P. Jearanaikoon, D. Perez-Guaita, B.R. Wood, Infrared spectroscopy coupled to cloud-based data management as a tool to diagnose malaria: A pilot study in a malaria-endemic country, Malar. J. 18 (2019) 348. https://doi.org/10.1186/s12936-019-2945-1.

[173] D. Zhang, X. Zhang, R. Ma, S. Deng, X. Wang, X. Wang, X. Zhang, X. Huang, Y. Liu, G. Li, J. Qu, Y. Zhu, J. Li, Ultra-fast and onsite interrogation of Severe Acute Respiratory Syndrome Coronavirus 2 (SARS-CoV-2) in waters via surface enhanced Raman scattering (SERS), Water Res. 200 (2021) 117243. https://doi.org/10.1016/j.watres.2021.117243.

[174] S.A. Bustin, V. Benes, J.A. Garson, J. Hellemans, J. Huggett, M. Kubista, R. Mueller, T. Nolan, M.W. Pfaffl, G.L. Shipley, J. Vandesompele, C.T. Wittwer, The MIQE guidelines: Minimum information for publication of quantitative real-time PCR experiments, Clin. Chem. 55 (2009) 611–622. https://doi.org/10.1373/clinchem.2008.112797.

[175] B.R. Wood, K. Kochan, D.E. Bedolla, N. Salazar-Quiroz, S.L. Grimley, D. Perez-Guaita, M.J. Baker, J. Vongsvivut, M.J. Tobin, K.R. Bambery, D. Christensen, S. Pasricha, A.K. Eden, A. Mclean, S. Roy, J.A. Roberts, J. Druce, D.A. Williamson, J. McAuley, M. Catton, D.F.J. Purcell, D.I. Godfrey, P. Heraud, Infrared Based Saliva Screening Test for COVID-19, Angew. Chemie - Int. Ed. 60 (2021) 17102–17107. https://doi.org/10.1002/anie.202104453.

[176] V. Schorer, J. Haas, R. Stach, V. Kokoric, R. Groß, J. Muench, T. Hummel, H. Sobek, J. Mennig, B. Mizaikoff, Towards the direct detection of viral materials at the surface of protective face masks via infrared spectroscopy, Sci. Reports 2022 121. 12 (2022) 1–9. https://doi.org/10.1038/s41598-022-06335-z.

[177] V.G. Barauna, M.N. Singh, L.L. Barbosa, W.D. Marcarini, P.F. Vassallo, J.G. Mill, R. Ribeiro-Rodrigues, L.C.G. Campos, P.H. Warnke, F.L. Martin, Ultrarapid On-Site Detection of SARS-CoV-2 Infection Using Simple ATR-FTIR Spectroscopy and an Analysis Algorithm: High Sensitivity and Specificity, Anal. Chem. 93 (2021) 2950–2958. https://doi.org/10.1021/acs.analchem.0c04608.

[178] M.S. Nogueira, L.B. Leal, W. Macarini, R.L. Pimentel, M. Muller, P.F. Vassallo, L.C.G. Campos, L. dos Santos, W.B. Luiz, J.G. Mill, V.G. Barauna, L.F. das C. e. S. de Carvalho, Rapid diagnosis of COVID-19 using FT-IR ATR spectroscopy and machine learning, Sci. Rep. 11 (2021) 1–13. https://doi.org/10.1038/s41598-021-93511-2.

[179] B.R. Wood, D.E. Bedolla, K. Kochan, D.I. Godfrey, D.F.J. Purcell, P. Heraud, Comment on Ultrarapid On-Site Detection of SARS-CoV-2 Infection Using Simple ATR-FTIR Spectroscopy and an Analysis Algorithm: High Sensitivity and Specificity, Anal. Chem. 93 (2021) 16974–16976. https://doi.org/10.1021/acs.analchem.1c03099.

[180] S.T. Kazmer, G. Hartel, H. Robinson, R.S. Richards, K. Yan, S.J. van Hal, R. Chan, A. Hind, D. Bradley, F. Zieschang, D.J. Rawle, T.T. Le, D.W. Reid, A. Suhrbier, M.M. Hill, Pathophysiological Response to SARS-CoV-2 Infection Detected by Infrared Spectroscopy Enables Rapid and Robust Saliva Screening for COVID-19, Biomedicines. 10 (2022). https://doi.org/10.3390/BIOMEDICINES10020351.

[181] L. Zhang, M. Xiao, Y. Wang, S. Peng, Y. Chen, D. Zhang, D. Zhang, Y. Guo, X. Wang, H. Luo, Q. Zhou, Y. Xu, Fast Screening and Primary Diagnosis of COVID-19 by ATR-FT-IR, Anal. Chem. 93 (2021) 2191–2199. https://doi.org/10.1021/acs.analchem.0c04049.

[182] G. Yin, L. Li, S. Lu, Y. Yin, Y. Su, Y. Zeng, M. Luo, M. Ma, H. Zhou, L. Orlandini, D. Yao, G. Liu, J. Lang, An efficient primary screening of COVID-19 by serum Raman spectroscopy, J. Raman Spectrosc. 52 (2021) 949–958. https://doi.org/10.1002/jrs.6080.

[183] Z. Zhang, D. Li, X. Wang, Y. Wang, J. Lin, S. Jiang, Z. Wu, Y. He, X. Gao, Z. Zhu, Y. Xiao, Z. Qu, Y. Li, Rapid detection of viruses: Based on silver nanoparticles modified with bromine ions and acetonitrile, Chem. Eng. J. 438 (2022) 135589. https://doi.org/10.1016/J.CEJ.2022.135589.

[184] P.C. Matthews, M.I. Andersson, C. V. Arancibia-Carcamo, K. Auckland, J.K. Baillie, E. Barnes, T. Beneke, S. Bibi, T. Brooks, M. Carroll, D. Crook, K. Dingle, C. Dold, L.O. Downs, L. Dunn, D.W. Eyre, J. Gilbert Jaramillo, H. Harvala, S. Hoosdally, S. Ijaz, T. James, W. James, K. Jeffery, A. Justice, P. Klenerman, J.C. Knight, M. Knight, X. Liu, S.F. Lumley, A.L. McNaughton, A.J. Mentzer, J. Mongkolsapaya, S. Oakley, M.S. Oliveira, T. Peto, R.J. Ploeg, J. Ratcliff, M.J. Robbins, D.J. Roberts, J. Rudkin, R.A. Russell, G. Screaton, M.G. Semple, D. Skelly, P. Simmonds, N. Stoesser, L. Turtle, S. Wareing, M. Zambon, SARS-CoV-2 RNA detected in blood products from patients with COVID-19 is not associated with infectious virus, Wellcome Open Res. 5 (2020). https://doi.org/10.12688/wellcomeopenres.16002.2.

[185] C.C.S. Bandeira, K.C.R. Madureira, M.B. Rossi, J.F. Gallo, A.P.M.A. da Silva, V.L. Torres, V.A. de Lima, N.K. Júnior, J.D. Almeida, R.M. Zerbinati, P.H. Braz-Silva, J.A.L. Lindoso, H. da Silva Martinho, Micro-Fourier-transform infrared reflectance spectroscopy as tool for probing IgG glycosylation in COVID-19 patients, Sci. Reports 2022 121. 12 (2022) 1–13. https://doi.org/10.1038/s41598-022-08156-6.

[186] M. Akdeniz, F. Uysal Ciloglu, C.U. Tunc, U. Yilmaz, D. Kanarya, P. Atalay, O. Aydin, Investigation of mammalian cells expressing SARS-CoV-2 proteins by surface-enhanced Raman scattering and multivariate analysis, Analyst. 147 (2022) 1213–1221. https://doi.org/10.1039/D1AN01989A.

[187] R. Kalkeri, Z. Cai, S. Lin, J. Farmer, Y. V. Kuzmichev, F. Koide, Sars-cov-2 spike pseudoviruses: A useful tool to study virus entry and address emerging neutralization escape phenotypes, Microorganisms. 9 (2021) 1744. https://doi.org/10.3390/microorganisms9081744.

[188] J. Sitjar, H.Z. Xu, C.Y. Liu, J.R. Wang, J. Der Liao, H.P. Tsai, H. Lee, B.H. Liu, C.W. Chang, Synergistic surface-enhanced Raman scattering effect to distinguish live SARS-CoV-2 S pseudovirus, Anal. Chim. Acta. 1193 (2022) 339406.

https://doi.org/10.1016/J.ACA.2021.339406.

[189] J.M. Condor Capcha, G. Lambert, D.M. Dykxhoorn, A.G. Salerno, J.M. Hare, M.A. Whitt, S. Pahwa, D.T. Jayaweera, L.A. Shehadeh, Generation of SARS-CoV-2 Spike Pseudotyped Virus for Viral Entry and Neutralization Assays: A 1-Week Protocol, Front. Cardiovasc. Med. 7 (2021) 381. https://doi.org/10.3389/fcvm.2020.618651.

[190] F. Bonnier, A.D. Meade, S. Merzha, P. Knief, K. Bhattacharya, F.M. Lyng, H.J. Byrne, Three dimensional collagen gels as a cell culture matrix for the study of live cells by Raman spectroscopy, Analyst. 135 (2010) 1697–1703. https://doi.org/10.1039/c0an00060d.

[191] A. Park, P. Hong, S.T. Won, P.A. Thibault, F. Vigant, K.Y. Oguntuyo, J.D. Taft, B. Lee, Sendai virus, an RNA virus with no risk of genomic integration, delivers CRISPR/Cas9 for efficient gene editing, Mol. Ther. - Methods Clin. Dev. 3 (2016) 16057. https://doi.org/10.1038/mtm.2016.57.

[192] S. Abdul-Rasool, B.C. Fielding, Understanding Human Coronavirus HCoV-NL63~!2009-11-13~!2010-04-09~!2010-05-25~!, Open Virol. J. 4 (2010) 76–84. https://doi.org/10.2174/1874357901004010076.

[193] E.N. Hoen, T. Cremer, R.C. Gallo, L.B. Margolis, Extracellular vesicles and viruses: Are they close relatives?, Proc. Natl. Acad. Sci. U. S. A. 113 (2016) 9155–9161. https://doi.org/10.1073/pnas.1605146113.

[194] M. Hassanpour, J. Rezaie, M. Nouri, Y. Panahi, The role of extracellular vesicles in COVID-19 virus infection, Infect. Genet. Evol. 85 (2020) 104422. https://doi.org/10.1016/j.meegid.2020.104422.

[195] W.A. Wells, When is a virus an exosome?, J. Cell Biol. 162 (2003) 960. https://doi.org/10.1083/jcb1626rr1.

[196] A. Gualerzi, S. Niada, C. Giannasi, S. Picciolini, C. Morasso, R. Vanna, V. Rossella, M. Masserini, M. Bedoni, F. Ciceri, M.E. Bernardo, A.T. Brini, F. Gramatica, Raman spectroscopy uncovers biochemical tissue-related features of extracellular vesicles from mesenchymal stromal cells, Sci. Rep. 7 (2017) 1–11. https://doi.org/10.1038/s41598-017-10448-1.

[197] A. Gualerzi, S.A.A. Kooijmans, S. Niada, S. Picciolini, A.T. Brini, G. Camussi, M. Bedoni, Raman spectroscopy as a quick tool to assess purity of extracellular vesicle preparations and predict their functionality, J. Extracell. Vesicles. 8 (2019) 1568780. https://doi.org/10.1080/20013078.2019.1568780.

[198] H. Zhang, A.C. Silva, W. Zhang, H. Rutigliano, A. Zhou, Raman Spectroscopy characterization extracellular vesicles from bovine placenta and peripheral blood mononuclear cells, PLoS One. 15 (2020) e0235214. https://doi.org/10.1371/journal.pone.0235214.

[199] Z.J. Smith, C. Lee, T. Rojalin, R.P. Carney, S. Hazari, A. Knudson, K. Lam, H. Saari, E.L. Ibañez, T. Viitala, T. Laaksonen, M. Yliperttula, S. Wachsmann-Hogiu, Single exosome study reveals subpopulations distributed among cell lines with variability related to membrane content, J. Extracell. Vesicles. 4 (2015). https://doi.org/10.3402/jev.v4.28533.

[200] S.G. Kruglik, F. Royo, J.M. Guigner, L. Palomo, O. Seksek, P.Y. Turpin, I. Tatischeff, J.M. Falcón-Pérez, Raman tweezers microspectroscopy of: Circa 100 nm extracellular vesicles, Nanoscale. 11 (2019) 1661–1679. https://doi.org/10.1039/c8nr04677h.

[201] J. Mihály, R. Deák, I.C. Szigyártó, A. Bóta, T. Beke-Somfai, Z. Varga, Characterization of extracellular vesicles by IR spectroscopy: Fast and simple classification based on amide and C[sbnd]H stretching vibrations, Biochim. Biophys. Acta - Biomembr. 1859 (2017) 459–466.

Declaration of interests

☒ The authors declare that they have no known competing financial interests or personal relationships that could have appeared to influence the work reported in this paper.

☐ The authors declare the following financial interests/personal relationships which may be considered as potential competing interests: